Morphological and electrophysiological properties of lateral deutocerebral cells in desert locust *Schistocerca gregaria*

Inaugural-Dissertation
to obtain the academic degree
Doctor rerum naturalium (Dr. rer. nat.)

submitted to the Department of Biology, Chemistry and Pharmacy
of Freie Universität Berlin

by

SERGEJ HARTFIL
from Podtessowo

2016

Die Arbeit wurde von April 2012 bis Januar 2016 unter der Leitung von Prof. Dr. Hans-Joachim Pflüger am Institut für Neurobiologie angefertigt.

1. Gutachter: Prof. Dr. Hans-Joachim Pflüger
2. Gutachter: Prof. Dr. Paul A. Stevenson

Datum der Disputation: 14.06.2016

Danksagung

Zunächst möchte ich dem Prof. Dr. Hans-Joachim Pflüger dafür danken, dass er mir die Möglichkeit gab in seiner Forschergruppe zu arbeiten, diese Arbeit betreute und das Equipment bereitgestellte.

Prof. Dr. Paul A. Stevenson möchte ich für die Begutachtung dieser Arbeit danken, für die Betreuung während des Aufenthalts in Leipzig und für den großzügigerweise ausgeliehen A/D-Wandler.

Heike Wolfenberg danke ich für das Aufrechterhalten der Ordnung und der freundlichen Atmosphäre im Labor. Zudem möchte ich ihr und Dr. Jan Rillich für die tatkräftige Unterstützung beim Ansetzen der Backfills danken.

Dr. Jessika Erdmann danke für die Unterstützung beim Erstellen dieser Arbeit. Ebenso danke ich ihr, Leonard Nadler und Konstantin Lehmann für die fachliche Kompetenz und die großartige Arbeitsatmosphäre.

Anschließend möchte ich meiner Familie für die Unterstützung danken.

Table of Contents

List of Tables

TABLE **Page**

List of Figures

FIGURE **Page**

1 Introduction

Among the neurohormones and neuromodulators in insects the monoamines octopamine (β,4-dihydroxyphenethylamine) and tyramine (4-hydroxyphenethylamine) fill an unique niche. Octopamine and tyramine were considered as invertebrate-specific amines for a long time, starting with the discovery in the posterior salivary glands of 3 different *Octopus* species (Erspamer, 1948; Esparmer and Boretti, 1951). Recent studies identified trace amine associated receptors in vertebrates (Lewin, 2008), but their role remains vague and not comparable to the role they play in invertebrates. They are suspected to be involved in a number of mental disorders, like schizophrenia in humans (Vladimirov et al., 2007) and show some vascular effects, among with the ability to increase blood pressure and heart rate (Rev: Broadley, 2010).

In insects, octopamine plays various roles, acting as neurotransmitter, neurohormone and neuromodulator (Orchard, 1982). It is in general considered being similar to catecholamines adrenaline and noradrenaline in vertebrates (Rev: Pflüger and Stevenson, 2005). Two classes of octopaminergic receptors are so far identified in insects: OCTα-R and OCTβ-R, with 3 receptor subtypes in the OCTβ-R class (Rev: Farooqui, 2012). All of them belong to the family of G-protein-coupled receptors (CPCRs) raising intracellular cAMP (OCTβ-R) or Ca^{2+} and to a lesser extent cAMP (OCTα-R) levels.

Prominent examples of octopaminergic cells in insects are dorsal and ventral unpaired median neurones (DUM, VUM) (Plotnikova, 1969). Most of them are octopaminergic, however, a subpopulation of GABAergic DUM cells was found in locust (Stevenson, 1999). Octopaminergic DUM/VUM neurones were identified and, in most works, researched in locust species *Locust migratoria* and *Schistocerca greagaria*. As their name suggests, they are located on the ventral or dorsal side of all ganglia, excluded the brain, with big soma in the middle of the ganglion, situated anteriorly or posteriorly. Most DUM cells are efferent, forming bilateral axons which enter peripheral nerves. Several works were done on DUM cells, enlightening their role in flight by regulating the glycolytic rate in flight muscles in the initial period of flight (Orchard and Lange, 1984; Duch and Pflüger, 1999; Mentel et al., 2003), initialising fat mobilisation in the

fat body directly (Van Marrewijk et al., 1980; Orchard et al., 1982) and orchestrating release of adipokineitc hormones I and II (AKHI, II) in the corpora cardiaca for prolonged periods of flight (Orchard et al., 1993; Van der Horst et al., 2001). Additionally, they were shown to have some effect with octopamine acting as neuromodulator by increasing the amplitude (Evans and O'Shea, 1977) and the relaxation rate of twitch tension (Evans and Siegler, 1982) in the extensor-tibiae hind leg muscle in locust, modulating the response strength of tactile strand hair receptors (Bräunig and Eder, 1998) and the forewing stretch receptor (Ramirez and Orchard, 1990). DUM cells were shown to use octopamine as neurotransmitter, too. The reproductive system in locust and *Drosophila melanogaster* is influenced by octopamine. In locust, octopamine steers the contraction of oviductal muscle (Orchard and Lange, 1985) and *Drosophila melanogaster* mutants, lacking tyramine beta-hydroxylase (Tβh), were shown to be unable to lay eggs (Monastirioti, 2003).

Other notable examples of octopamine being involved in physiology of insects are regulation of the heart rate in the larvae of hawk moths *Manduca sexta* (Platt and Reynolds, 1986) and *Agrius convolvuli* (Matsushita et al., 2002), initiation of luminescence in firefly *Photuris versicolor* (Christensen and Carlson, 1982) and increase of ventilation rate in the dobsonfly *Corydalus cornutus* (Bellah et al., 1984) and desert locust *Locusta migratoria* (Armstrong et al., 2006).

Furthermore, in insects, octopamine is involved in flight or fight response, aggression and stress. Increased levels of octopamine in the haemolymph of crickets are associated with aggression (Adamo et al., 1995). However, it was argued later that octopamine mediates aggression most likely with release sites in the central nervous system (CNS) (Stevenson, 2005), not in the haemolymph. Heat stress and food deprivation in locusts, unspecific stress in the cockroach *Periplaneta americana* are associated with increased levels of octopamine in the haemolymph and CNS (Armstrong et al., 2006; Davenport and Evans, 2008; Hirashima and Eto, 1993), though the role of octopamine in the stress response in still not completely clear. Especially, in the fruit fly *Drosophila melanogaster* increased levels of octopamine correspond with stress, but are not the cause of the stress response (Gruntenko et al., 2004). Visual sensory input is influenced by octopaminergic cells, too. A population of octopaminergic cells in the median deutocerebrum of locust was shown to be involved in dishabituation of the descending contralateral movement detector (DCMD) (Bacon et al., 1995).

While most of the works dealing with the role of octopamine in insects concentrate on physiology, some octopaminergic neurones were found to play an important role in appetitive learning. In the honeybee *Apis melifera* the octopaminergic ascending neurone VUMmx1 was shown to reinforce the unconditional stimulus pathway (Hammer, 1993). More recent studies in the fruit fly confirmed the role of octopamine in the sugar reward reinforcement (Schwaerzel et al., 2003).

The synthesis of octopamine starts with the amino acid tyrosine (4-hydroxyphenylalanine), which is transformed by tyrosine decarboxylase (TDC) to tyramine. In the next step tyramine is transformed to octopamine by tyramine β-hydroxylase (Tβh). For a long time tyramine never got any attention other than being a metabolic precursor of octopamine. However, recent studies showed, that it plays a role on its own as neurotransmitter and neuromodulator. One of earlier findings on the role of octopamine was tracing the distribution of octopamine and tyramine in the CNS of *Locusta migratoria*. It was shown that the distribution of tyramine in the CNS is lower than that of octopamine, and higher levels of tyramine compared to octopamine were found in skeletal muscles (Downer et al., 1993). Some years later, a null-mutant at the Tβh was created in *Drosophila melanogaster*, allowing to experiment on animals which lack octopamine completely (Monastirioti et al., 1996).

However, the role of tyramine is still not known well. Two receptors, called TYR1-R and TYR2-R with a higher affinity to tyramine than to octopamine were identified (Rev: Farooqui, 2012). Both of them are G-protein-coupled receptors, with TYR1-R lowering intracellular cAMP level in response to higher concentrations of tyramine or raising intracellular Ca^{2+} level in response to higher concentration of octopamine and tyramine-only receptor TYR2-R, raising intracellular Ca^{2+} level.

Tyraminergic-only cells were found in the larval CNS of *Drosophila melanogaster* (Nagaya, 2002) and it was found, that *hono*-mutants, lacking tyraminergic receptors, show deficits in olfaction and lack of inhibition in excitatory junction potentials (EJP) in larval body muscles compared to flies, lacking octopamine and control group (Kutsukake et al., 2000). Tyramine was showed to be involved in egg laying in *Drosophila melanogaster* (Cole et al., 2005) and some evidence for tyraminergic neurones innervating the oviduct in the locust *Locusta migratoria* was found (Donini and Lange, 2004). Mutants, lacking TDC show reduced locomotion in *Drosophila melanogaster* compared to Tβh mutants (Hardie et al., 2007) and show decrease in flight initiation probability,

which may by rescued by blocking tyraminergic receptors (Brembs et al., 2007).

Even though some of these effects may exist only due to the fact, that Tβh mutants accumulate big amounts of tyramine instead of octopamine, with octopaminergic receptors showing affinity to high concentrations of tyramine, a strong indication exists for tyramine being an independent neurotransmitter and neuromodulator.

Due to the importance of octopamine and tyramine in the CNS of insects, efforts were made to map the distribution of octopaminergic and tyraminergic cells. In desert locust *Schistocerca gregaria* the main source of octopamine in the suboesophageal (SOG), thoracic and abdominal ganglia are unpaired median neurones (Rev: Bräunig and Pflüger, 2001). The brain lacks unpaired median cells, however, some DUM interneurones from the SOG are projecting into the brain (Braunig, 1991) and intrinsic octopaminergic cell populations in the brain were identified (Konings et al., 1988). In a more recent work, distribution of tyraminergic cells was mapped in desert locust *Schistocerca gregaria*, using anti-tyramine and anti-octopamine antibodies (Kononenko et al., 2009). Among purely tyraminergic cells, a bilateral dorsolateral deutocerebral cluster named OA3/TA was mapped, consisting of four pairs of cells. Cells of this cluster showed tyraminergic-only immunoreactivity in animals, immediately put on ice before dissection and following immunohistochemistry. If animals were subjects to unspecific stress for 15 min, cells of the OA3/TA cluster additionally showed anti-octopamine immunoreactivity.

In this study, cells of the dorsolateral cluster are analysed with intracellular recordings for the first time with respect to their spiking properties, response to stimulation and neuroanatomy. Additionally, backfills from abdominal connectives were performed to address the question whether these cells are local to the brain or descend further in the nerve cord. This question was of particular interest, since most DUM cells in locust are efferent and project in peripheral nerves of the ganglion where soma of the particular cell is situated. Furthermore, anti-horseradish peroxidase (HRP) stainings were done to verify the position and size of the dorsolateral cluster.

2 Material and methods

2.1 Dissection

2.1.1 Animals

For experiments with dissection adult *Schistocerca greagaria* of both sexes in gregarious phase from Blades biological Ltd. (UK, Edenbridge) were used. The animals were kept crowded, with a 12 hours day/night cycle, at 28 °C and 10% air humidity. Prior to all experiments animals were cooled down to 4 °C for 15 min.

2.1.2 Dissection for retrograde staining with neurobiotin

The animal was fixated on a dish and the abdomen was opened dorsally. One of the connectives between the forth and fifth abdominal ganglia was cut and embedded into a small vaseline pool. The pool was filled with distilled water for 5 min, then its content was switched with 5% neurobiotin-distilled water solution. Afterwards the animal was left at 4°C for four to five days before applying the immunohistochemical protocol.

2.1.3 Dissection for staining with horseradish peroxidase

By a cooled down animal wings, mouthparts and legs were cut. The animal was fixed using needles with the dorsal side upwards on a platform made of modelling clay. A needle was put through the head capsule frontally between both antennal nerves to stabilise the head. The pronotum was cut off, exposing the head and thorax. The dorsal side of the head capsule was opened behind the antennae, going backwards and down along the edge of the compound eyes. The resulting piece of cuticle was severed with scissors from the side to cut through the mandibles. In the semi-open head, the loose gut was pulled out of the head, tentorium was cut on the ends and removed together with the remaining loose parts of the mandibles. Then the connectives to the suboesophageal ganglion were cut and the brain was removed out of the head capsule.

2.1.4 Dissection for anterograde staining with neurobiotin

The dissection for anretrograde stainings with neurobiotin resembles the dissection for stainings with horseradish peroxidase. In this dissection the legs were kept and fixed with modelling clay on a platform to prevent movements. After removing the tentorium and mandibles a platform, made of an injection needle and covered with wax, was placed under the brain in the resulting cavity and pulled up, so the brain rested on it. The remaining cavities between the platform and the head capsule were filled with petroleum jelly (Molyduval GmbH, Germany) to seal the brain and form a bath for the ringer solution.

2.1.5 Ringer solution

For perfusion an isotonic ringer solution was used (protocol developed by Heinar in the laboratory of Dr. Prof. H.-J. Pflüger), consisting of 150 mM NaCl (Carl Roth, Karlsruhe, Germany), 10 mM HEPES (Sigma-Adlrich, St. Louis, USA), 25 mM sucrose (Carl Roth, Karlsruhe, Germany) , 5 mM KCl (Carl Roth, Karlsruhe, Germany), 5 mM $CaCl_2$ (Carl Roth, Karlsruhe, Germany) and 2 mM $MgCl_2$ (Carl Roth, Karlsruhe, Germany). All compounds were diluted in distilled water and adjusted to an pH value of 7.4 with NaOH.

2.2 Immunocytochemistry and histochemistry

2.2.1 Histochemistry for stainings with Neurobiotin

The nerve cord was dissected out of the animal and fixated in a 4% paraformaldehyde (PFA) solution, and dehydrated for 10 min in solution with increasing ethanol concentration (50, 70, 90 and 100%), transferred for 2×5 min to methyl salicylate, and rehydrated in a solution with an decreasing ethanol concentration (100, 90, 70 and 50%). Preparations which were not immediately scanned with the confocal microscope, were stored in 70% ethanol. Otherwise, after rehydrating in 50% ethanol solution the preparation was washed for 3×20 min in 0.1 M phosphate buffer (PB, pH = 7.4) + 1% Triton X-100 solution and pre-incubated in Triton X-100 (Linaris GmbH, Drossenheim, Germany) with 10% normal goat serum in 0.1 M PB + 1% Triton X-100. For the next step the tissue was incubated in 1% streptavidin-Cy2 fluorescent dye (Dianova GmbH, Hamburg, Germany), diluted in 0.5% in 0.1 M PB + 1% Triton X-100. After incubation in darkness

at room temperature for 12 hours, the preparation was washed for 3×10 min in 0.1 M PB and dehydrated in solutions with increasing ethanol concentrations (50, 70, 90 and 100%), each step for 10 min. Dehydrated preparations were put into 1:1 solution of 100% ethanol and methyl salicylate, to be cleared and covered on a slide in methyl salicylate.

2.2.2 Anti-octopamine/anti-tyramine/neurobiotin whole mount

Anti-octopamine/anti-tyramine whole mounts were performed in preparations of *Schistocerca gregaria*. Specificity of octopamine antibodies on locust species *Schistocerca gregaria* and *Locusta migratoria* was confirmed in several previous works on brain tissue, suboesophageal, thoracic and abdominal ganglia (Konings et al., 1988; Braunig, 1991; Stevenson et al., 1992). The issue of the specificity of the tyramine antibody and its crossreactivity with octopamine is discussed in detail by Kononenko et al. (2009).

The dissected nerve cord was fixated for 3 hours at room temperature in a solution consisting of 1% glutaraldehyde and 1% PFA, both solved in 0.1 M PB. After fixation, the nerve cord was washed in a solution of 0.1 M PB for 15 min. Then the nerve cord was dehydrated in solutions with ascending ethanol contents (50, 70, 90% ethanol for 10 min, 100% ethanol for 2×5 min), put in xylol for 2×4 min and rehydrated in solutions with descending contents of ethanol (90, 70, 50% for 10 min each). After that treatment, the nerve cord was placed in 0.1 M PB solution at 37°C for 10 min, then for 30 min in 0.1% collagenase/dispase (Roche Diagnostics, Mannheim, Germany) + 0.1% hyaluronidase (Sigma-Adlrich Chemie GmbH, Munich, Germany) in 2 ml of the 0.1 M PB solution at the same temperature. Then the nerve cord was washed in 0.1 M PB solution for 15 min. In following steps, the nerve cord was put in a 1% sodium borohydride solution, dissolved in 0.1 M PB for 10 min on the shaker, following 15 min in 0.1 M PB solution, and 4×15 min in 0.1 M PB + 1% Triton X-100 (Sigma-Adlrich, St. Louis, USA). In the next step, the nerve cord was preincubated for one hour in 10% normal goat serum (Linaris GmbH, Drossenheim, Germany) diluted in 0.1 M PB + 1% Triton X-100 solution and incubated for 5 days at 4 °C on shaker in 1 ml of solution consisting of following primary antibodies: 0.1% anti-octopamine antibody (Jena Bioscience, Jena, Germany) and 0.2% anti-p-tyramine antibody (Merck Chemicals, Darmstadt, Germany) diluted in 0.1 M PB + 1% Triton X-100 + 1% sodium azide (NaN_3). After treatment with primary antibody the nerve cord was washed in 0.1 M PB + 1% Triton X-100 for 6×20 min and left in dark for 12 hours on shaker by room temperature in the solution consisting of secondary antibodies with an attached fluorescent dye (1% Cy3-conjugated

goat anti-mouse + 1% Cy2-conjugated goat anti-rabbit) and 0.5% streptavidin-Cy5 for amplification of neurobiotin (all from Dianova GmbH, Hamburg, Germany), diluted in 1% TritonX-100. All of the following steps took place in dark, to prevent bleaching of the fluorescent dye. The nerve cord was rinsed in 0.1 M PB solution for 3×20 min and an ascending ethanol solution (50, 70, 90, 100%, every step for 10 min). Then, after being placed in a 1:1 solution, consisting of 100% ethanol and methyl salicylate, the tissue was cleared in pure methyl salicylate and covered with a microscope slide.

2.2.3 Anti-horseradish peroxidase

Anti-horseradish peroxidase (anti-HRP) whole mounts were done on dissected nerve cord of adult *Schistocerca gregaria* which was previously fixated in 1% glutaraldeyde and 2% PFA both solved in 0.1 M phosphate buffer (PB, pH = 7.4). After fixating the tissue was washed for 3×15 min in 0.1 M PB and dehydrated in solutions with ascending ethanol contents (50, 70, 90 and 100% ethanol in distilled water for 10 min each). The tissue was cleared for 5 min in xylol, rehydrated in solutions with descending ethanol contents (100, 90, 70, 50% for 10 min each) and washed in 0.1 M PB at 37 °C for 10 min. After washout the tissue was placed for 1 hour at 37 °C in 0.1% collagenase/dispase (Roche Diagnostics, Mannheim, Germany) + 0.1% hyaluronidase (Sigma-Adlrich Chemie GmbH, Munich, Germany) in 2 ml of the 0.1 M PB solution with a following washouts in 0.1 M PB for 10 min, 1% sodium borohydride in 0.1 M PB for 10 min on a shaker and in 0.1 M PB + 1% Triton X-100 (Sigma-Aldrich, St.Louis, USA) for 4×15 min. Subsequently, the tissue was pre-incubated in 10% normal goat serum (Linaris GmbH, Drossenheim, Germany) solved in 0.1 M PB + 1% Triton X-100 on a shaker and washed out for 3×20 min 0.1 M PB + 1% Triton X-100. After that treatment the Goat anti-HRP-Cy3 (Dianova GmbH, Hamburg, Germany) antibody was applied in proportion 1:500, solved in 0.1 M PB + 0.5% Triton X-100 and incubated over night in dark on a shaker. The following day tissue was washed out in 0.1 M PB for 3×15 min, dehydrated in solutions with ascending ethanol content (50, 70, 90 and 100% for 10 min each), placed in a solution consisting of 1 part methyl salicylate and 1 equal part of 100% ethanol for 10 min and cleared in methyl salicylate for 30 min before being covered with a microscope slide.

2.3 Intracellular recordings

2.3.1 Intracellular recording and staining

Intracellular recordings were performed with an Axoclamp 2B intracellular amplifier (former Axon Instruments, now Molecular Devices, USA) using an Axon Instruments HS-2-x0.1L headstage. The electrodes were pulled with a P–97 puller (Sutter Instruments Co., USA) from borosilicate glass (BF100–50–7.5, Sutter Instruments Co., USA), resulting in electrodes with a final resistance of 60–100 MΩ, then filled with 2.5% neurobiotin in 2 M potassium chloride solution. Neurobiotion tracer (Vector Laboratories LTD., UK) was used as tracer (Kita and Armstrong, 1991). It was allowed to pull up by capillary forces into the tip of the electrode. The remaining space in the electrode was filled up with a 2 M KCl solution using a fine needle, leaving a bubble of air between the neurobiotin solution and the potassium chloride solution, to prevent dilution of the neurobiotion. The electrode tip was directed at the dorsolateral deutocerebrum in an location where the position of the soma was suspected.

Data was acquired with a CED Micro 1401 Mk II using Spike2 software (Cambridge Electronic Design Limited, Cambridge, UK). After doing intracellular recordings the target cell it was filled with neurobiotin by applying a depolarising current of 2-5 nA, sometimes up to 9 nA in electrodes with lower resistance, to iontophoretically convey neurobiotin into the cell. A Grass SD-9 square pulse stimulator (Natus Neurology Inc. - Grass Products, Warwick, USA) was used to drive the "step activate"-channel of the Axoclamp 2B intracellular amplifier with 200 ms long pulses delivered at frequency of 4 Hz. Current injection was monitored with the Axoclamp 2B intracellular amplifier. In most cases, determined by the stability of the recording, the cell was filled in a time range of 30 min up to 1 hour. Afterwards the nerve cord was dissected, left in ringer solution for 12 hours, then the histochemistry protocol for neurobiotin was applied as described in (2.2.1).

2.3.2 Sensory stimulation

All experiments were performed in a semi-intact preparation, with an opened head capsule, partially opened thorax, removed mouthparts and wings. Stimulation was done while simultaneously performing an intracellular recording, as described in (2.3.1). The start of the stimulation was marked in the recording software manually with an remote electrical trigger. Mechanical stimulations were done with a fine paintbrush. The indi-

cated body part was stroked gently for approximately 0.5 sec. Antennae and all legs were stroked dorsal from proximal to distal direction resulting in stimulation of the femur, tibia and tarsus in legs. Cerci were stimulated with upside-down strokes. Abdomen and thorax were stimulated with lateral movements in posterior direction with respect to the body axis. Visual stimulation was performed with a white paper disk, attached to a stick. It was moved starting in the frontal part of the visual field of the animal in longitudinal direction for approximately 1 sec. Acoustic stimulation was done with short rattling of a bunch of keys, producing a high-pitch sound. For every method of stimulation several repeated stimulations were performed. The responses of impaled neurones in the brain to the according stimuli were recorded and evaluated later. After performing the stimulation trials, the impaled cell was stained, as described in detail in (2.3.1).

2.4 Confocal microscopy and image processing

Confocal microscopy was performed with a Leica Microsystems (Wetzlar, Germany) SP2 confocal microscope. For overview scans, a Leica HC PL APO 10×0.4 IMM UV objective was used. Detail scans were done using a Leica HCX APO L U-V-I 20×0.5 W UV water immersion objective. All scans were performed with a scan resolution of 1024 x 1024 pixels. The selected step size on the Z-axis was depending on objective used: 2.4 μm for the HC PL APO 10×0.4 IMM UV objective and 1.4 μm for the HCX APO L U-V-I 20×0.5 W UV objective. Fluorescent dyes were excited by using one of the available lasers: Ar/Kr-Laser at 488 nm and two He/Ne-Lasers with a wavelength of 543 and 633 nm. If the preparation was stained with multiple fluorescent dyes images were scanned in sequential mode to prevent cross-excitation.

Image processing of confocal scans was done in Fiji (Schindelin et al., 2012). Stack image files, acquired with Leica SP2 confocal microscope were loaded into software and collapsed as a Z-projection to a desired projection plane. The colours were inverted for better visibility and a scale bar was added using the file metadata provided by the confocal microscope. All images were aligned so the cell body of the stained cell can be found on the right side of picture. In anatomical images, the orientation refers to the embryonic axis. Most images were darkened in Pixelmator (Pixelmator Team Ltd., Vilnius, Lithuania) for better visibility of structures. Arrows and descriptions were added to the image file in Illustrator (Adobe Systems, San Jose, U.S.).

2.5 Data analysis and generation of plots

Spike overlay figures were plotted with GNU Octave (John W. Eaton David Bateman and Wehbring, 2014) using the original electrophysiological recordings and a spike train of 10 successive spikes. Spike duration and spike amplitude were measured manually in Spike2, by setting horizontal and vertical cursors for 12 successive spikes. This data was imported and plotted in R, a freely available statistics software package (R Core Team, 2016). Analysis of ISI (interspike interval) was done in R with exported spike trains, using R-package STAR (Pouzat and Chaffiol, 2009). ISI histogram was done with the same package, where a best fit model for a given distribution of ISIs was chosen manually and applied, so that bin width is set automatically as if the fitted distribution was true. Spike train examples of spontaneous spiking and bursts after a stimulation were done with an exported trace from Spike2 in Illustrator (Adobe Systems, San Jose, U.S.). Measurements of the cell body size were done by loading the confocal scans in Fiji and measuring the cells by fitting ellipses, resulting in two values, describing the size of a cell body: *Major*, the longest distance in an ellipse, and *Minor*, the shortest distance in an ellipse. This data was exported to R and plotted as xy-plot for all evaluated scans. Plots, showing response to stimulation were done with a self-written script in R by counting the number of spikes one second before the onset of stimulation (pre-trial) and one second after the onset of stimulation (trial). These number were then expressed in Hertz (Hz) and plotted as a barplot, where two bars represent the mean frequency in Hz of all pre-trials and trials for every applied method of stimulation and error bars show the standard deviation of the mean frequency separately for the pre-trials and trials.

2.6 Numbers of evaluated preparations

Immunoctyochemical preparations with anti-octopamine/anti-tyramine, combined with retrograde tracing with neurobione were done in a total number of N=5. However, only 2 of them showed acceptable level of staining and were evaluated. Anti-HRP stainings were done in a total of N=8 preparations. All of them were evaluated. Intracellular single-cell recordings were done in large number of preparations. Only those, where the size of cell bodies and neuroanatomy in the brain met certain criteria (size, position in the brain, quality of staining in the brain, suboesophageal and thoracic ganglia) were evaluated, resulting in a total number of 5 different cells with N=1 each. These cells (DLC Type I-V) are discussed in the following.

3 Results

3.1 Retrograde stainings with neurobiotin

Five retrograde histochemical stainings with neurobiotin ("backfills"), inserted through the cut in the ipsilateral connective between forth and fifth abdominal ganglia, were performed in adult animals to find out whether cells of the OA3/TA group, as described by Kononenko et al. (2009) descend to the abdominal ganglia. Additionally, an anti-octopamine/anti-tyramine protocol was performed on the nerve tissue. Most of the cells, stained with neurobiotin either arborize ipsilateral in lateral protocerebrum or have cell bodies and axons located around the central complex, ipsi- and contralateral. In two preparations out of five four cells in the dorsolateral cluster were stained with neurobiotin (fig: 3.2.a, 3.1.a). In both introduced preparations these cells were stained on the ipsilateral side of the brain with respect to the cut connective.

In the first stained preparation, four cells were stained with neurobiotin on the left side of the brain. Additionally, three cells in the location of the dorsolateral cluster were stained with anti-octopamine and anti-tyramine antibodies (fig: 3.1.c, 3.1.b). Two of them are on the left side and are cells, co-stained with neurobiotin (fig: 3.1.d). Their cell bodies have a size of approximately 30 μm on the major axis and 20 μm on the minor axis. Additionally, one cell is stained with anti-tyramine and anti-octopamine on the other side of the brain. It has a size of 34 μm on the major and 24 μm on the minor axis.

In the second preparation 4 cells were stained with neurobiotin on the left side of the brain (fig: 3.2.a). Two of them show some weak co-localisation with anti-octopamine and anti-tyramine (fig: 3.2.d). However, it is most likely due to auto-fluorescence of the tissue, since no cell-shaped objects can be found on the left side on images corresponding to anti-octopamine and anti-tyramine stainings. (fig: 3.2.c, 3.2.b). Three cell bodies were stained with both anti-octopamine and anti-tyramine on the left side of the brain. Their cell bodies are sized similarly to cell bodies of cells, stained with neurobiotin, with a major-axis being ca. 40-42 μm long. (fig: 3.3.a:2nd backfill OA/TA, 2nd backfill NB).

Generally, the backfills confirm previous findings regarding octopaminergic cell in the dorsolateral part of the brain. Up to four cells with cell bodies in the dorsolateral cluster were found to descend in the ipsilateral connective, regarding position of the cell body, to, at least, the 5th abdominal ganglion. Previous findings show, that in retrograde stainings done more anterior in the nerve cord up to 5 cells in the dorsolateral cluster can be stained (Willer, 2010; Ina Sohm(unpublished results)).

Other notable octopaminergic cells clusters, stained with in these preparations include the protocerebral medulla 4 (PM4) cells, as described by Stern et al. (1995).

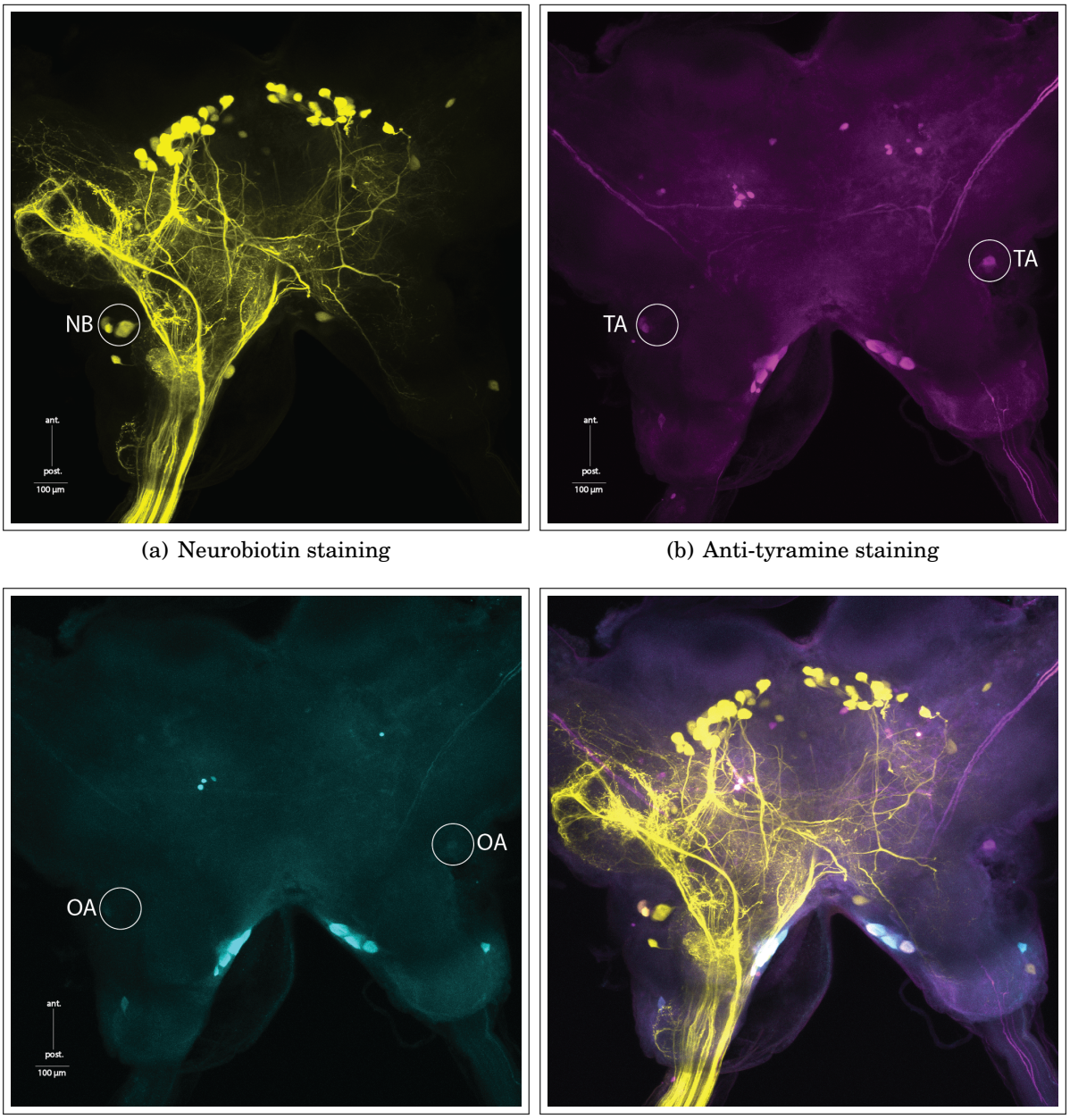

(a) Neurobiotin staining

(b) Anti-tyramine staining

(c) Anti-octopamine staining

(d) Composite of three stainings

Figure 3.1: (a) Neurobiotin staining, **(b)** anti-tyramine staining, **(c)** anti-octopamine staining, **(d)** composite of all three stainings in a single brain preparation combined with neurobiotin backfills between the 4th and 5th abdominal ganglia. Yellow – neurobiotin, magenta – anti-tyramine, cyan - anti-octopamine. Abbreviations: NB – neurobiotin, OA – octopamine, TA – tyramine.

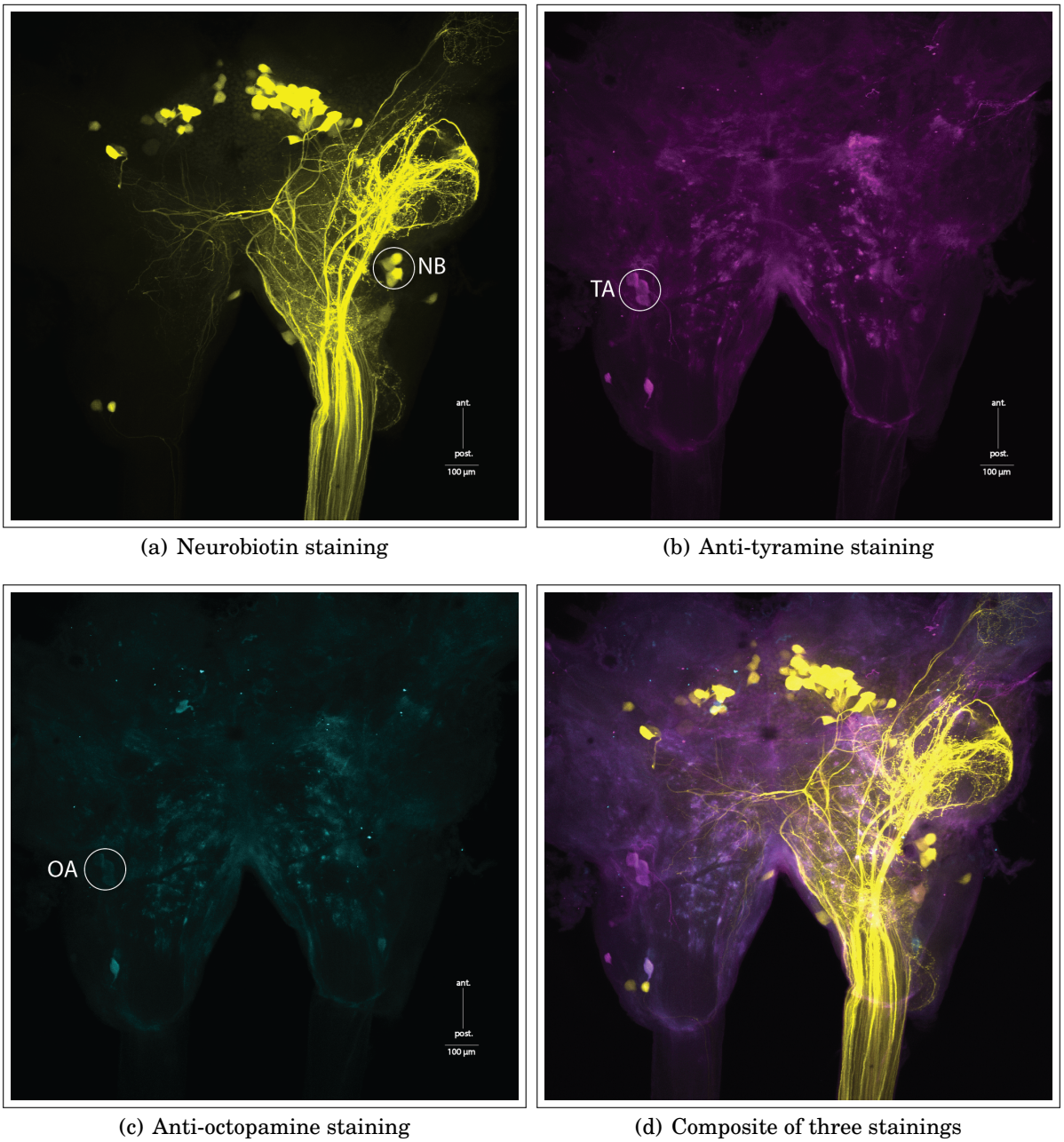

(a) Neurobiotin staining

(b) Anti-tyramine staining

(c) Anti-octopamine staining

(d) Composite of three stainings

Figure 3.2: (a) Neurobiotin staining, **(b)** anti-tyramine staining, **(c)** anti-octopamine staining, **(d)** composite of all three stainings in a single brain preparation combined with neurobiotin backfills between the 4th and 5th abdominal ganglia. Yellow – neurobiotin, magenta – anti-tyramine, cyan - anti-octopamine. Abbreviations: NB – neurobiotin, OA – octopamine, TA – tyramine.

3.2 Anti-HRP stainings

In order to find out, how many cells with sizes, corresponding to size of cell bodies stained with neurobiotin in retrograde stainings between the 4. and 5. abdominal ganglia are situated in the dorsolateral cluster in the brain of locust, anti-HRP stainings were performed in dissected brains of *Schistocerca gregaria* in a total of 8 animals. In these preparations dorsolateral clusters were evaluated by measuring the size of cells, if possible, on the left and right sides of the brain, resulting in a total of 12 evaluated clusters.

The dorsolateral cluster (hereafter referred to as "DLC") is located in the lateral deutocerebrum between a lateral protocerebral cluster and a lateral cluster of cells in the protocerebrum (fig: 3.3.b). Up to 204 cells were counted in preparations scanned with the best resolution available.

Cell size was measured in 8 preparations stained with HRP resulting in a total of 12 DLC cluster being evaluated. Size was measured using ellipses, thus resulting in two parameters describing the size of a cell: *Major*, the longest distance between two points in an ellipse and *Minor*, the shortest distance (fig: 3.3.a). Cells within DLC vary strongly in their size, with smallest values being 6.4 μm on the *Major* axis and 3.9 μm on the *Minor* axis. The biggest cells in the cluster reach the size of 39.4 μm on the *Major* axis and 27 μm on the *Minor* axis. However, the mean cell size in the DLC cluster is notably smaller with 16.2 and 11.3 μm on the *Major* and *Minor* axes respectively.

Judged by size, the four cells, traced in two preparations (see 3.1) with retrograde neurobiotin stainings, and the three cells, stained with anti-octopamine/anti-tyramine antibodies in each of the preparatins are among the biggest cells in the DLC cluster since the majority of cells measured shows a notably smaller size. These cells are candidates for being the cells, stained in the intracellular recordings (see 3.3).

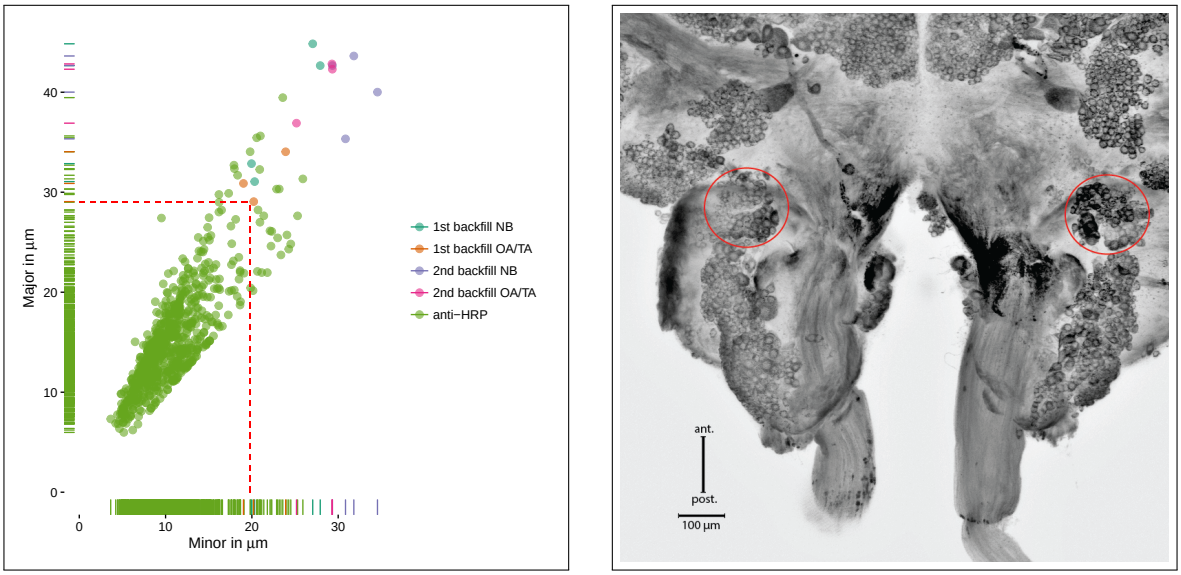

(a) Size of cells in the DLC cluster

(b) Location of the dorsolateral cluster

Figure 3.3: (a) Size of cells in the dorsolateral cluster. *Major* and *Minor* are the primary and secondary axis of the ellipse, fitting the cell body. Green dots stand for cells in anti-HRP stainings (731 cells measured in 12 dorsolateral clusters, in a total of 8 animals), red dots for cells, stained with neurobiotin backfills (4 cells in each of 2 preparations). Inside the block, build by red dashed lines are cells, which can be excluded from being candidates to octopaminergic cells based on the size of their cell body. **(b)** Anti-HRP staining in the brain in 10x magnification. Red circles mark the location of the dorsolateral cell cluster (DLC).

3.3 Descending cells of the dorsolateral cluster

To get insight into neuroanatomy and electrical properties of descending cells in the DLC, intracellular single cell recordings were performed in the dorsolateral cluster. Five descending cells were found and stained in the DLC. Each of these cells was recorded only once. These cells are labeled as DLC Type I-V.

3.3.1 DLC Type I

Neuroanatomy

The cell body of the DLC Type I cell is located in the deutocerebrum, anteriorly in relation to the antennal lobe. It has a slightly ellipsoid shape, stretched on the dorsoventral axis with a size of 32 and 26 μm on the major and minor axis respectively. The cell body forms an axon which branches out in two secondary branches in median deutocerebrum

(fig: 3.4). One of those branches forms a descending axon projecting towards the suboesophageal and thoracic ganglia. It splits into one secondary branch (fig: 3.4.a, 3.4.b:I), projecting downwards in a half-closed loop to the median part of the deutocerebrum splitting in several finer branches.

Another branch projects into anterior brain regions and forms four tertiary branches. Two of them are projecting anteriorly and ventrally (fig: 3.4.a, 3.4.b:III-IV), another pair projects anteriorly and dorsally (fig: 3.4.a, 3.4.b:V, VI). Branch III lays dorsally in posterior direction in the same deutocerebral region, as the branch I. Branches III and IV are projecting parallel in anterior direction and ventrally on the dorsoventral axis. They show an extensive arborization in the region where the peduncle of the mushroom body is located. Some of their smaller branches innervate the median region of the central complex (CC). Branches VIa, b are projecting in same anterior region as III and IV, but more laterally. Branch VIa projects in the peduncle of the mushroom body, VIb, c project in lateral protocerebrum, most likely in the area of the anterior optical tract. Branches Va, b project ventrally and laterally in optical tract posterior in relation to branch VIb. Branches VId and Vc are projecting dorsally within protocerebrum in the direction of the cell body. They arborize approximately in the region where axons of giant interneurones (GI) terminate (Boyan et al., 1989).

The axon of the cell descends towards the suboesophageal (SOG) and thoracic ganglion via the ipsilateral connective. In the SOG, it enters the ganglion on the ipsilateral side, regarding to the position of the cell body in the nerve cord, projects through the ganglion and exits it on the same side (fig: 3.5.a, 3.5.c). The axon branches out towards the middle of the SOG, in contralateral direction. On the way through the SOG it arborizes in five regions towards the midline of the ganglion in contralateral direction (marked as "ar." on the transverse projection). The axon lies within the dorsal intermediate tract (DIT) descending from the dorsal part of the tract to the ventral part on its way through the ganglion. According to its position, it innervates dorsal commissures of all three neuromeres fused to SOG: mandibular, maxillary and labial (Tyrer and Gregory, 1982).

Entering the prothoracic ganglion, the axon descends within the dorsal intermediate tract (DIT) and projects towards the dorsal region (fig: 3.5.b) where it arborizes in one stained branch towards the midline in contralateral direction and one smaller branch, which runs laterally. They branches project approximately in regions, where projections from the ventral mesothoracic chordotonal organs are reported (Hustert, 1978).

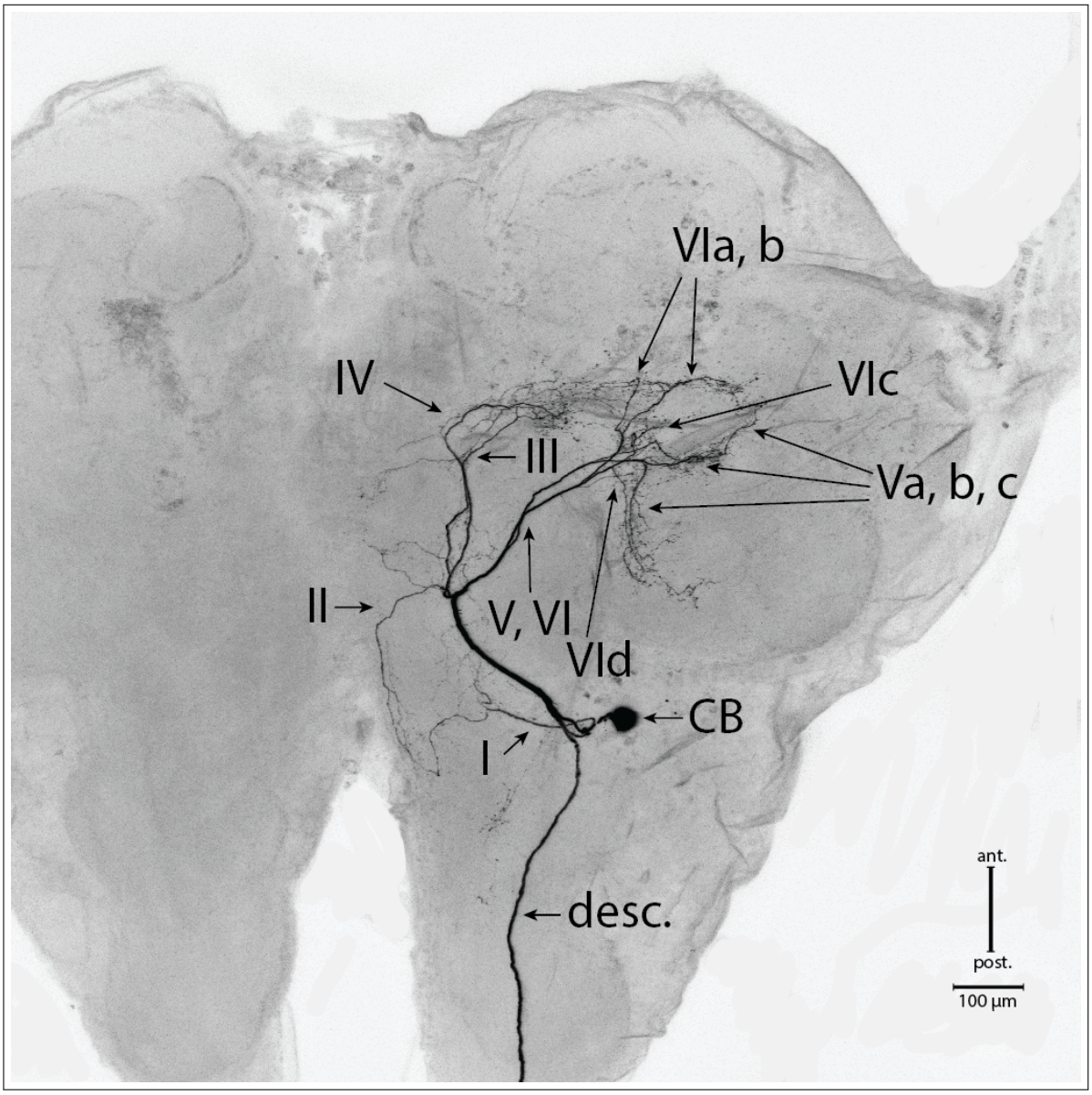

(a) Brain 10x magnification in transverse projection

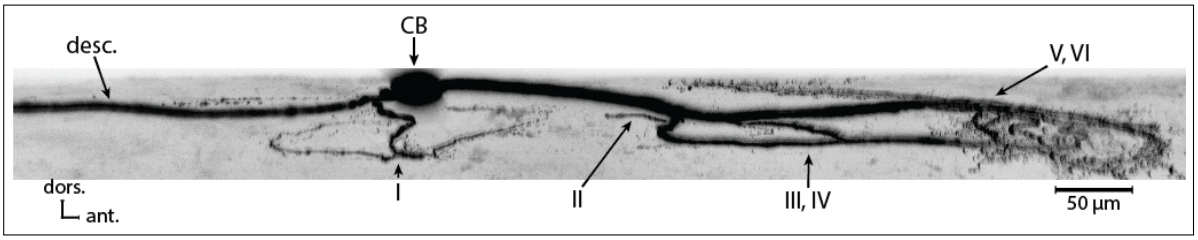

(b) Brain 20x magnification in sagittal projection

Figure 3.4: Projections of an intracellularly stained DLC Type I cell in the brain. **(a)** transverse projection of the brain in 10x magnification. **(b)** sagittal projection of the brain in 20x magnification. Abbreviations: I - VI are secondary branches in the brain, "desc." – descending axon, CB – cell body, ar. – arborization, ant. – anterior, post. – posterior.

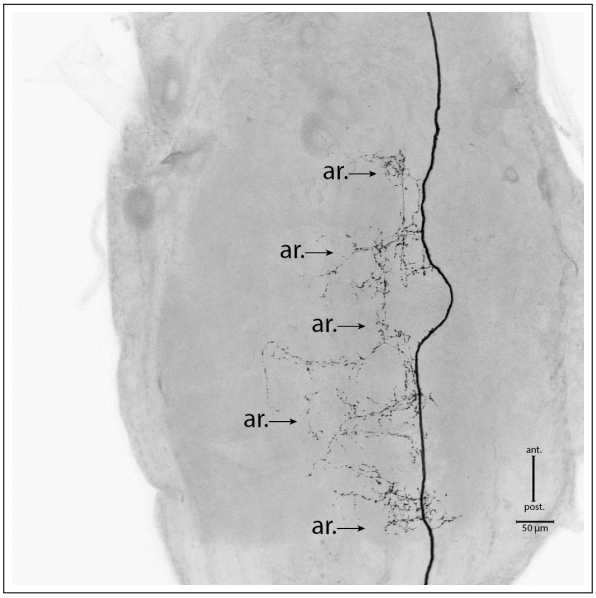

(a) SOG 20x magnification in transverse projection

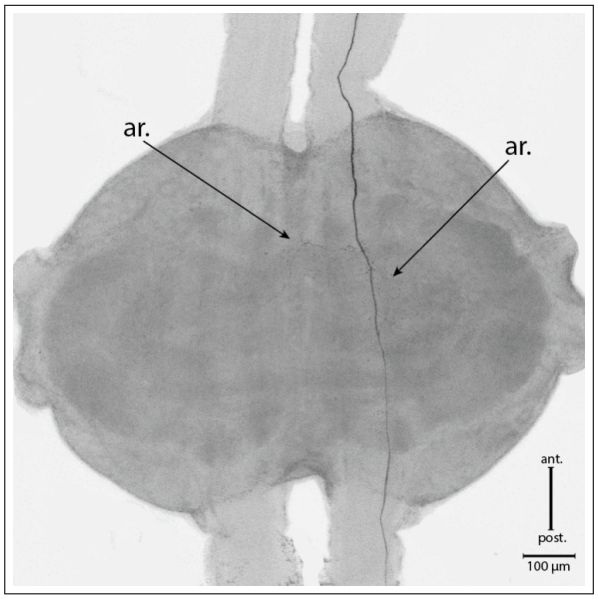

(b) Prothoracic ganglion 10x magnification in transverse projection

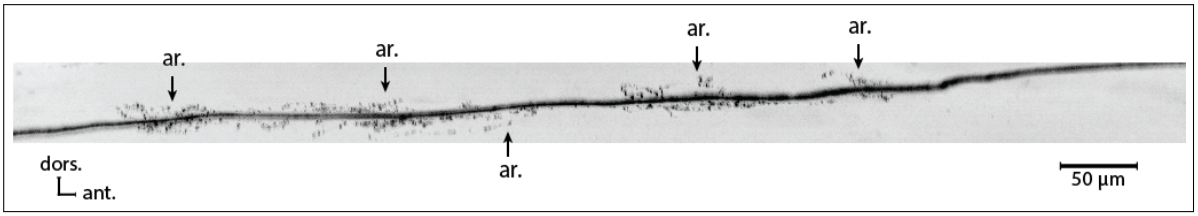

(c) SOG 20x magnification in sagittal projection

Figure 3.5: Projections of an intracellularly stained DLC Type I neurone in the suboesophageal and prothoracic ganglia. **(a)** Transverse projection of the suboesophageal ganglion, **(b)** transverse projection of the prothoracic ganglion, **(c)** sagittal projection of the suboesophageal ganglion. Projections are probably not stained entirely. Abbreviations: ar. – arborization, ant. – anterior, post. – posterior.

Electrophysiology and spike properties

The electrode was aimed at the location of the cell body in the dorsolateral cluster, thus the recordings occured most likely between the cell body and the junction. Cell of this type was recorded only once.

Spike shape was measured using 10 successive spikes of a DLC Type I cell before any mechanosensory stimulation was applied (fig: 3.6.a) . Cell has its resting potential at -50 mV and is characterized by large overshooting action potential with a spike initiation threshold of -45 mV.

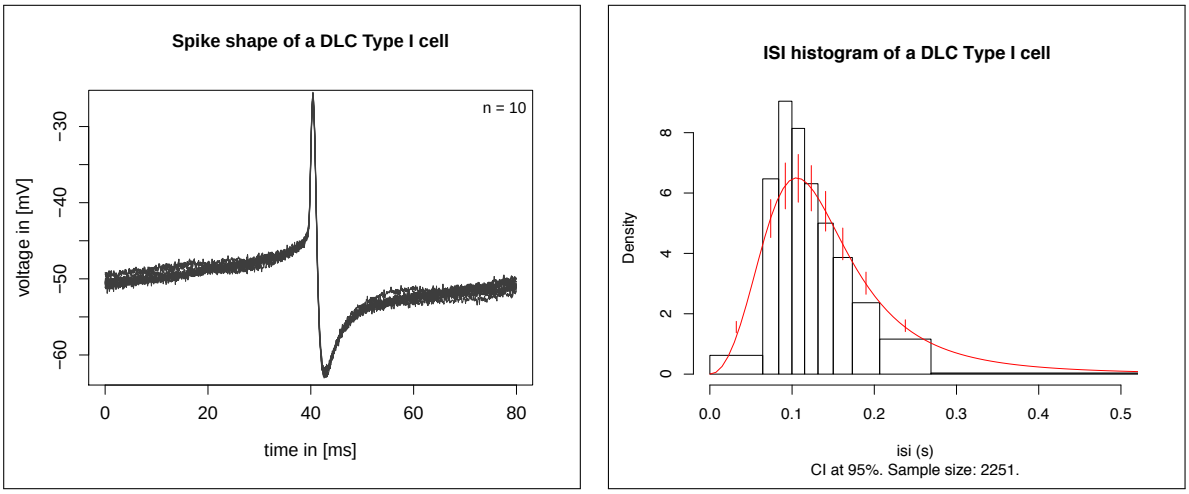

(a) Spike shape (b) Distribution of interspike invervalls

Figure 3.6: (a) A spike shape overdraw of a DLC Type I cell. 10 successive spikes were used to draw a shape. **(b)** Interspike interval histogram of an DLC Type I cell. Bin width was optimised using an fitted log-logistic probability distribution (red line) with variable bin width, so that 10% of the interspike interval fall into each bin. Red bars represent the 95% confidence interval (CI).

The duration of a spike, measured from the beginning of the depolarisation to the most negative potential of the hyperpolarization has a median of 3.38 ms (fig: 3.7.a) with a mean of 3.36 ms (SD = 1 ms, n = 12 successive spikes). Spikes have a median amplitude of 36.5 mV (mean = 36.5 mV, standard deviation = 0.51 ms, n=12) (fig: 3.7.b). The most negative measured value was -62.26 mV and the most positive -25.38 mV.

The cell shows a frequency spiking pattern with an interspike interval (ISI) in between 0.013 s (76.9 Hz) as shortest time period between 2 successive spikes, and 3.717 s (0.26 Hz) as longest time period. The mean ISI is 0.185 s (5.4 Hz) with a standard deviation of 0.246 s (fig: 3.6.b). This measurement includes periods, where no stimulation was applied, and periods where the animal was receiving mechanosensory stimulation.

Experiments were performed in a semi-intact animal, with open head, partially open thorax, removed mouthparts, wings and fixed legs. The cell recorded from was located on the left side of the body. This side is referred to as the ipsilateral side. The DLC Type I cell shows a rhythmic increase and decrease of the cell potential, most likely in phase with respiratory rhythm. The breathing frequency can vary in between 0.08 Hz and 4 Hz in locusts and is highly variable (Burrows, 1996). The experiments consisted of blocks of single repeated trials with one stimulation each. For each trial spikes were

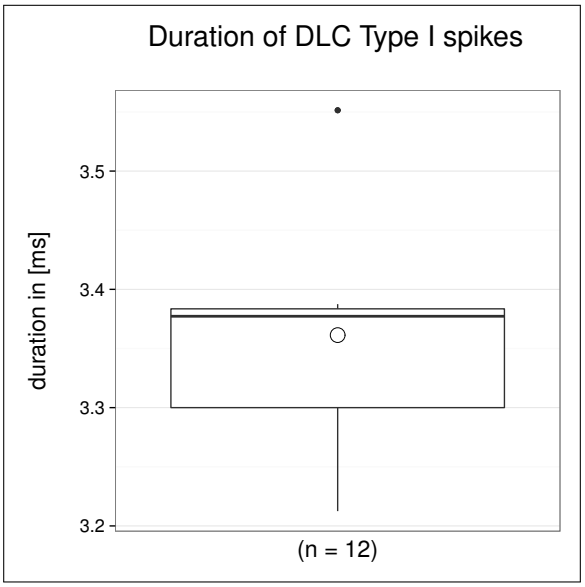

(a) Duration

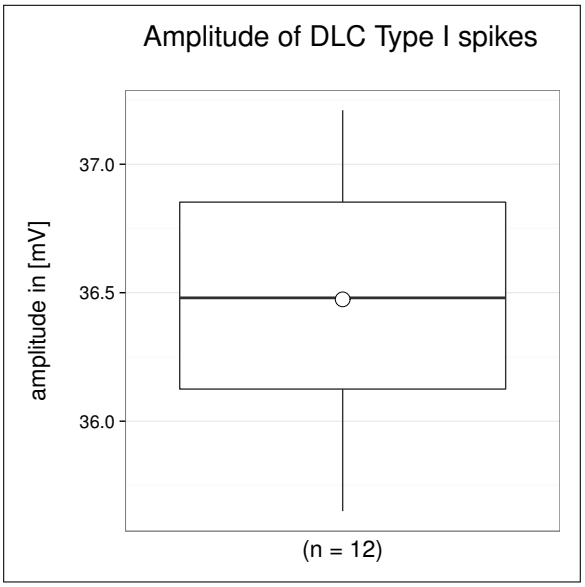

(b) Amplitude

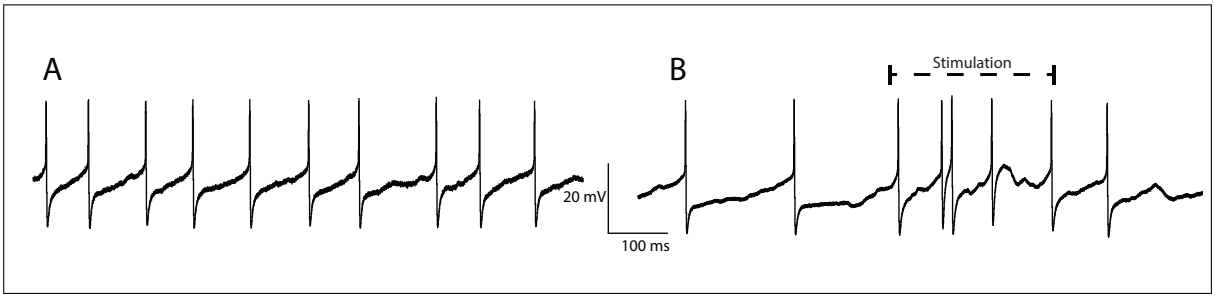

(c) Spiking pattern

Figure 3.7: Properties of a single DLC Type I cell. **(a)** Cumulative duration of 12 successive spikes, plotted as a boxplot. In boxplot, box represents the first and third quantiles, line in the middle of the box shows the median, white point stands for mean. Line represents the median (3.38 ms), dot represents the mean (3.36 ms). Standard deviation = 0.1 ms. **(b)** Cumulative amplitude of 12 successive spikes, plotted as a boxplot. Line represents the median (36.48 mV), dot represents the mean (36.47 mV). Standard deviation = 0.5 mV. **(c)** Intracellular recordings of a DLC Type I cell before (A) and after (B) tactile stimulus application to the ipsilateral (left) side of the abdomen.

counted in a second preceding the stimulation and the second after the stimulation. The difference between those number is the net response. In case of multiple trials in a block the mean and standard deviation of then net responses were calculated and plotted.

Tactile stimulation of the abdomen on both sides was sufficient to evoke short high-frequency bursts in the DLC Type I cell (fig: 3.8:abl, abr). Stimulation of the contralateral right side of the abdomen resulted in higher net difference in frequency.

An increase in spiking frequency after a tactile stimulation can be observed in the ipsilateral side of the thorax (fig: 3.8:tl). A decrease with a huge deviation could be observed on the contralateral side of the thorax, which indicates no or weak input (fig: 3.8:tr).

Both ipsi- and contralateral cerci were stimulated simultaneously (fig: 3.8:crc) and showed an increase in net spike frequency. The standard deviation is as high as the net increase in spike frequency after stimulation. This is maybe due to a rapid habituation to the tactile stimulus, since the number of spikes and spike frequency are declining with every subsequent trial (fig: 3.9.a). However, the possibility of stimulation of the posterior part of the abdomen by stimulation cerci and thus, an "overshadowing" of a possible cercal input can not be completely excluded.

No difference in spike frequency (fig: 3.8:snd) can be found in response to acoustic stimulation which was done by rattling a bound of metallic keys.

Tactile antennal stimulation did not increase the spike frequency of both ipsilateral and contralateral antennae (fig: 3.8:al, ar). Both show big deviation of the means with a small net decrease compared to pre-trial frequency.

Tactile stimulation of the ipsilateral and contralateral hind legs increased the net spike frequency (fig: 3.8:hll, hlr). However, it was not the case in all trials, which is indicated by a standard deviation, which is equal to the net response. The strength of response is declining in the 3rd trial in the ipsilateral hind leg (fig: 3.9.b) which may be due to differences of applied pressure or due to the habituation to the stimulus. The contralateral leg produces only up to two spikes in three of five trials and provides most likely no excitatory input to the DLC Type I cell (fig: 3.9.c).

The middle pair of legs showed similar results with either no net increase compared to the time of the pre-trial or a small net decrease of spike frequency on the ipsilateral

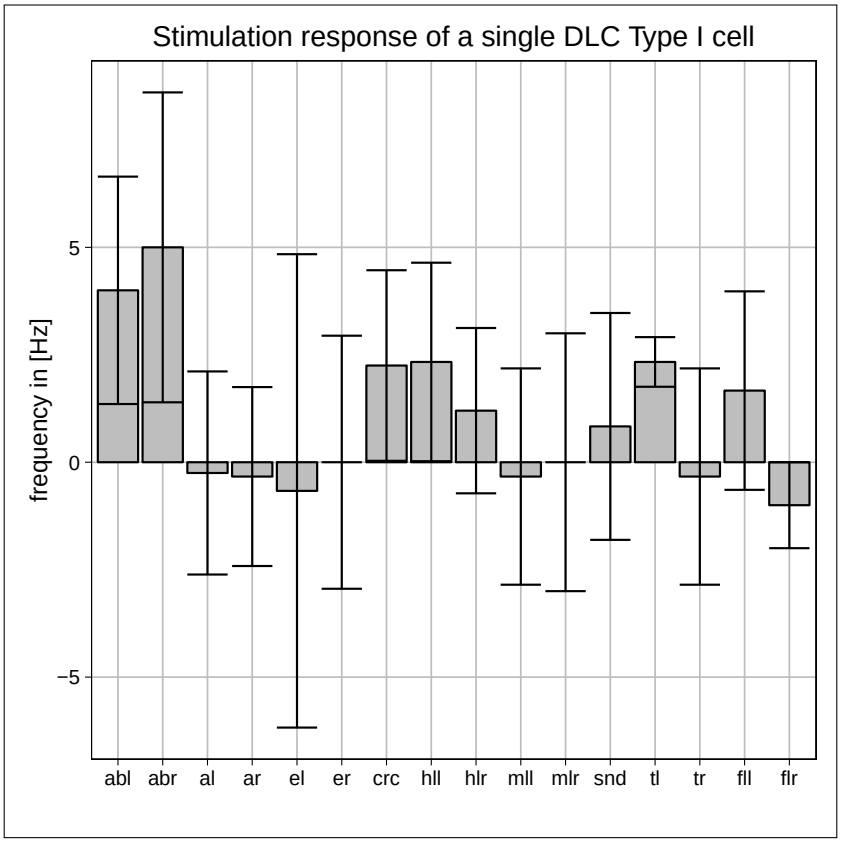

Figure 3.8: Response to stimulation of a single DLC Type I cell. Bars represent the mean frequency net difference between one second trial and one second pre-trial time in a trial block. Error bars represent a standard deviation of the mean net difference frequency for each trial block. Left side is the ipsilateral side of the body in relation to the location of the cell body in the brain, right side is the contralateral side of the body. Abbreviations: ABL – abdomen left (3 trials), ABR – abdomen right (3 trials), AL – antenna left (4 trials), AR – antenna right (3 trials), EL – eye left (3 trials), ER – eye right (4 trials), CRC – cerci (4 trials), HLL – hind leg left (3 trials), HLR – hind leg right (5 trials), MLL – mid leg left (3 trials), MLR – mid leg right (3 trials), SND – sound (6 trials), TL – thorax left (3 trials), TR – thorax right (3 trials), FLL – front leg left (3 trials), FLR – front leg right (3 trials).

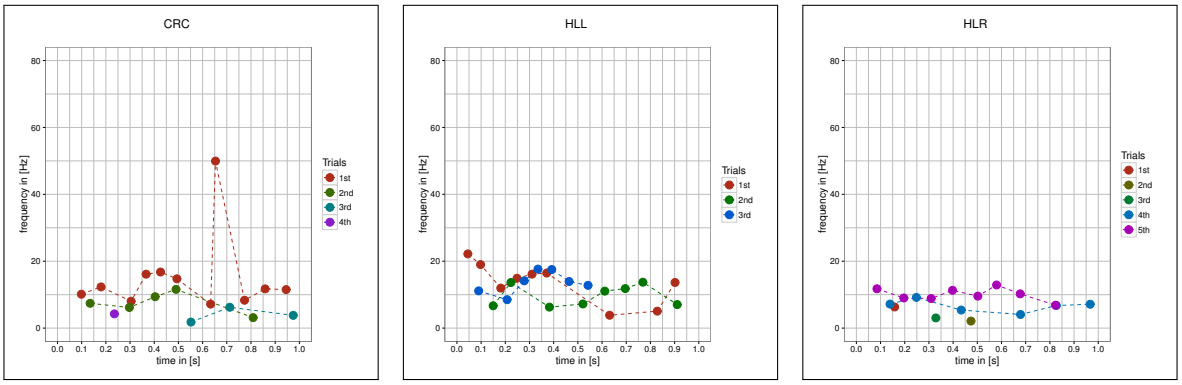

(a) Cerci (b) Ipsilateral hind leg (c) Contralateral hind leg

Figure 3.9: Instantaneous frequency in the 1 sec. trial period after tactile stimulation. Frequency in Hz is calculated between a pair of spikes using interspike intervals. Trials correspond to single trials in a trial block. **(a)** cerci, **(b)** ipsilateral hind leg, **(c)** contralateral hind leg.

side. (fig: 3.8mll, mlr). They most likely provide no input to the DLC Type I cell.

It is difficult to make a conclusion about a possible input from the frontmost pair of legs, where only the stimulation of the ipsilateral leg is sufficient to induce a slight increase of spike frequency in the DLC Type I cell and the contralateral leg even shows a slight decrease in net difference (fig: 3.8:fll, flr). Both show a big standard deviation, which is most likely due to the fact, that in each leg one of the three subsequent trials induced no spikes. This may have different reason. It can be due to the previously mentioned rhythmic activity of the DLC Type I cell. Another possibility is a weak input from the front legs with a rapid habituation.

Visual stimulation, performed with a white stimulation disk moved horizontally in the lateral visual field of the animal in a distance of approximately 5 cm, was not able to increase the deviation (fig: 3.8:el, er). These stimulations either provided no difference in net spike frequency (contralateral eye), or a small decrease accompanied with a big deviation which is most likely due to chance (ipsilateral eye).

Summing up, the DLC Type I cell responds with an increase of spike frequency after tactile stimulation of the ipsilateral side of the thorax and bilateral stimulation of the abdomen. It is not clear, whether there is a response to the tactile stimulation of both hind legs, cerci and frontmost leg pairs, since the response shows a high variability in frequency which may be due to a weak input or have other reasons which differ from

the provided stimulation.

3.3.2 DLC Type II

Neuroanatomy

The cell body of the DLC Type II cell is located dorsally in lateral deutocerebrum (fig: 3.10) and slightly stretched on the anterioposterior axis (fig: 3.10.c:CB). It measures 42.8 μm on its major and 30.6 μm on its minor axes. The cell body forms an axon which projects in the contralateral direction and forms a junction with two branches. One of them descends to the suboesophageal ganglion (fig: 3.10.a:desc.), other projects dorsal in contralateral direction, forming the three secondary branches (fig: 3.10.a:I - III).

Branch I (fig: 3.10.a:I) projects into the dorsal median part of the deutocerebrum. One of its branches projects into the direction of the lateral accessory lobe (LAL). Branch II (fig:3.10.a:II) splits up in four branches, every one of them forming several smaller branches. Most of them form projections in the fan-shaped body (CBU) and the lateral accessory lobe (LAL). Branch III (fig: 3.10.a:III) projects laterally into the protocerebrum, where it forms three smaller branches which terminate in the peduncle of the mushroom body.

An additional cell body was stained in the posterior part of the DLC cluster.

Within the suboesophageal ganglion (fig: 3.10.b) the axon of the cell projects within the lateral dorsal tract (LDT) (Tyrer and Gregory, 1982) without forming any notable arborizations. It enters the ganglion on the ipsilateral side with respect to the cell body and leaves it on the same side through the connective to the prothoracic ganglion.

In general DLC Type II cell shows less fine arborisation in the brain and SOG compared to DLC cells Type I (3.3.1), III (3.3.2), IV (3.3.4) and V (3.3.5). This is probably due to finer projections of the cell not being stained entirely.

Electrophysiology and spike properties

The cell was aimed at the location of the cell body in the dorsolateral cluster, thus the recordings occurred most likely between the cell body and the junction. Cell of this type was recorded only once.

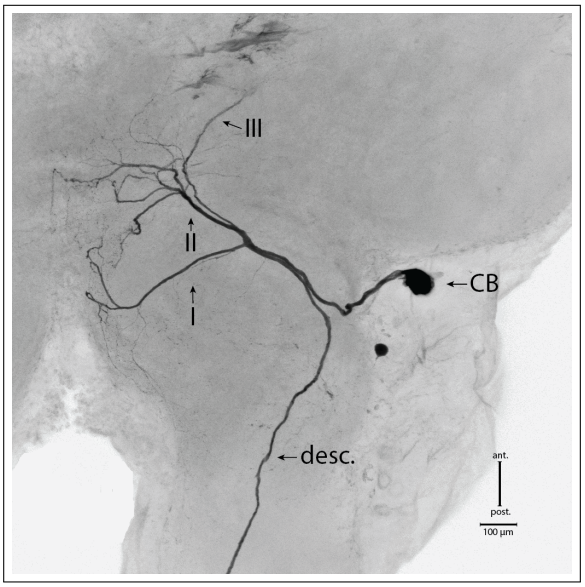

(a) Brain 20x magnification in transverse projection

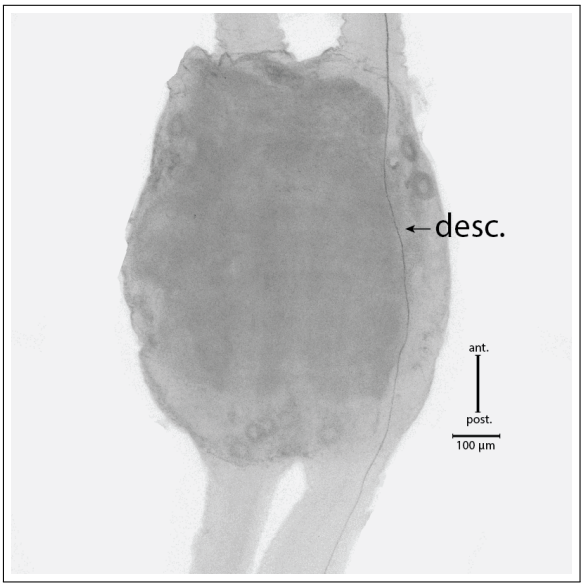

(b) SOG 10x magnification in transverse projection

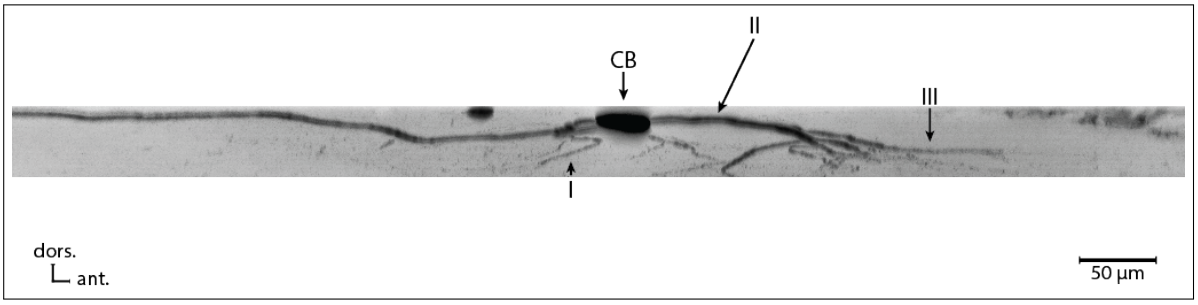

(c) Brain 20x magnification in sagittal projection

Figure 3.10: Projections of an intracellularly stained DLC Type II cell in the brain and suboesophageal ganglion. Additional cell body was stained in the posterior part of the dorolateral cluster. **(a)** Brain in transverse projection, **(b)** suboesophageal ganglion in transverse projection, **(c)** brain in sagittal projection. Projections are probably not stained entirely. Abbreviations: I - III are secondary branches in the brain, "desc." – descending axon, CB – cell body, ant. – anterior, post. – posterior, dors. – dorsal.

A spike shape overdraw was done using 10 successive spikes (fig: 3.11.a). Spikes are characterised through the large overshooting potential and prolonged period of hyperpolarization with a resting potential around -48 mV with a spike initiation threshold of -43 mV.

The duration of a single spike (fig: 3.11.c), measured from the onset to the most negative point of the hyperpolarization, has a median of 4.2 ms (mean = 4.28, SD = 0.1 ms, n = 12). The amplitude of a single spike(fig: 3.11.d) has a median of 59.88 mV (mean = 56.83 mV, SD = 0.56 mV, n = 12), with -11.2 mV as the most positive and -69.1 mV as the most negative potential.

The cell exhibits a slow frequency spiking pattern with an interspike interval (ISI) between 0.107 sec (9.34 Hz) as the shortest ISI and 7.475 sec (0.13 Hz) as the longest ISI (fig: 3.11.b). This includes times where the cell was stimulated. The mean ISI is 1.258 sec and its standard deviation is 0.991 sec, which is equivalent to an average spike frequency of 0.79 Hz.

Stimulations were performed in semi-intact animals, with opened head capsule, removed legs and eyes painted black to exclude visual cross-talking while stimulating the antennae. The cell body of the cell recorded from is located on the left side of the nerve cord. This side is referred to as the ipsilateral side.

The experiments consisted of blocks of single repeated trials with one stimulation each. For each trial spikes were counted in a second preceding the stimulation and the second after the stimulation. The difference between those number is the net response. In case of multiple trials in a block the mean and standard deviation of then net responses were calculated and plotted.

DLC Type II cell shows in general a rather low spiking frequency with most interspike intervals being in a range of 1 second (fig: 3.11.b).

Abdomen was stimulated with a stroke on a dorsal side without separate tests for the ipsi- and contralateral sides (fig: 3.12:ab). This stimulation was sufficient to increase the net spike frequency to 1 Hz compared to the spike frequency in the pre-trial. With the 0.6 Hz high standard deviation of means it should be assumed, that the DLC Type II cell receives excitatory mechanosensory input from the abdomen. However, it is not clear whether the received is bilateral since both sides were stimulated at the same

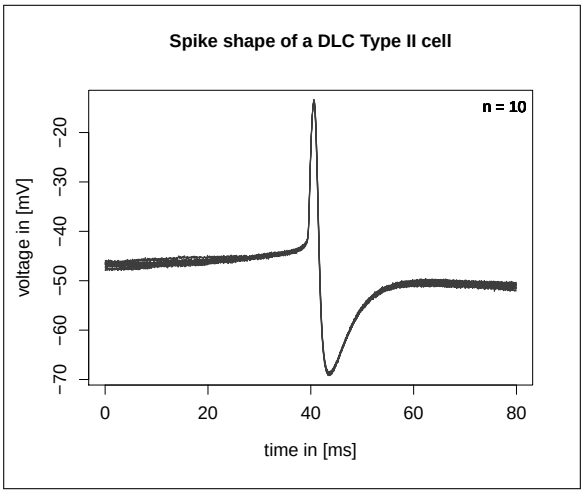

(a) Spike shape

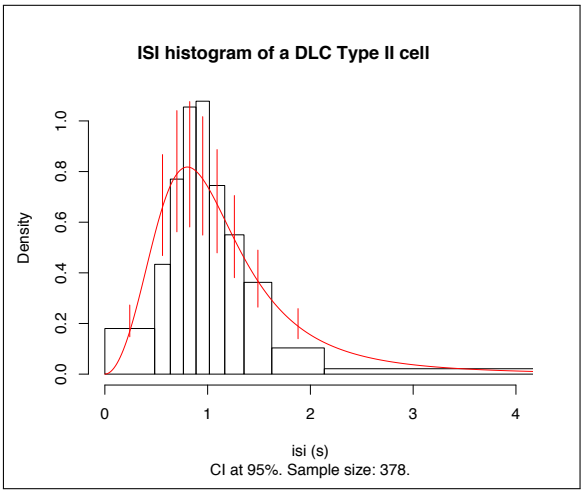

(b) Distribution of interspike intervalls

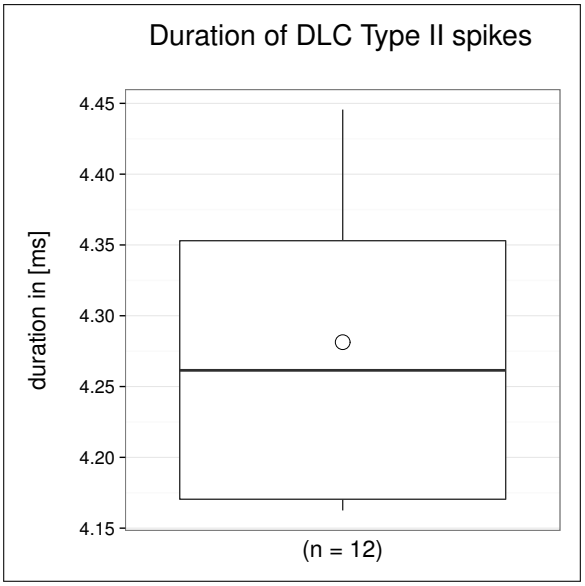

(c) Duration

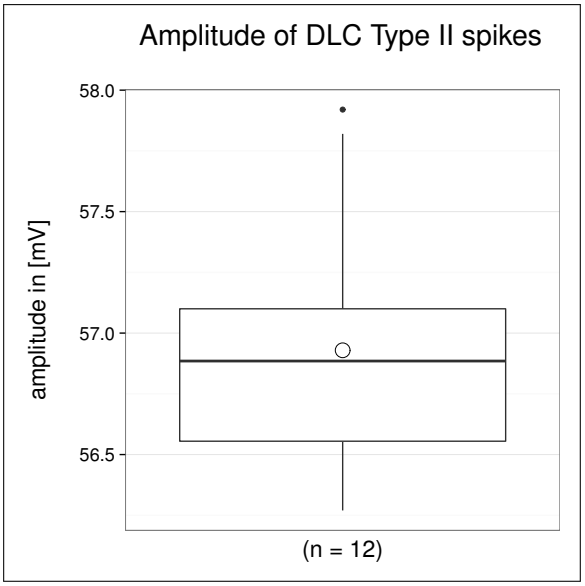

(d) Amplitude

Figure 3.11: (a) A spike shape overdraw of a DLC Type II cell. 10 successive spikes were used to draw a shape. **(b)** Interspike interval histogram of an DLC Type II cell. Bin width was optimised using an fitted log-logistic probability distribution (red line) with variable bin width, so that 10% of the interspike interval fall into each bin. Red bars represent the 95% confidence interval (CI). **(c)** Cumulative duration of 12 successive spikes, plotted as a boxplot. In boxplot, box represents the first and third quantiles, line in the middle of the box shows the median, white point stands for mean. Line represents the median (4.2 ms), dot represents the mean (4.28 ms). Standard deviation = 0.1 ms. **(d)** Cumulative amplitude of 12 successive spikes, plotted as a boxplot. Line represents the median (56.88 mV), dot represents the mean (56.83 mV). SD = 0.56 mV.

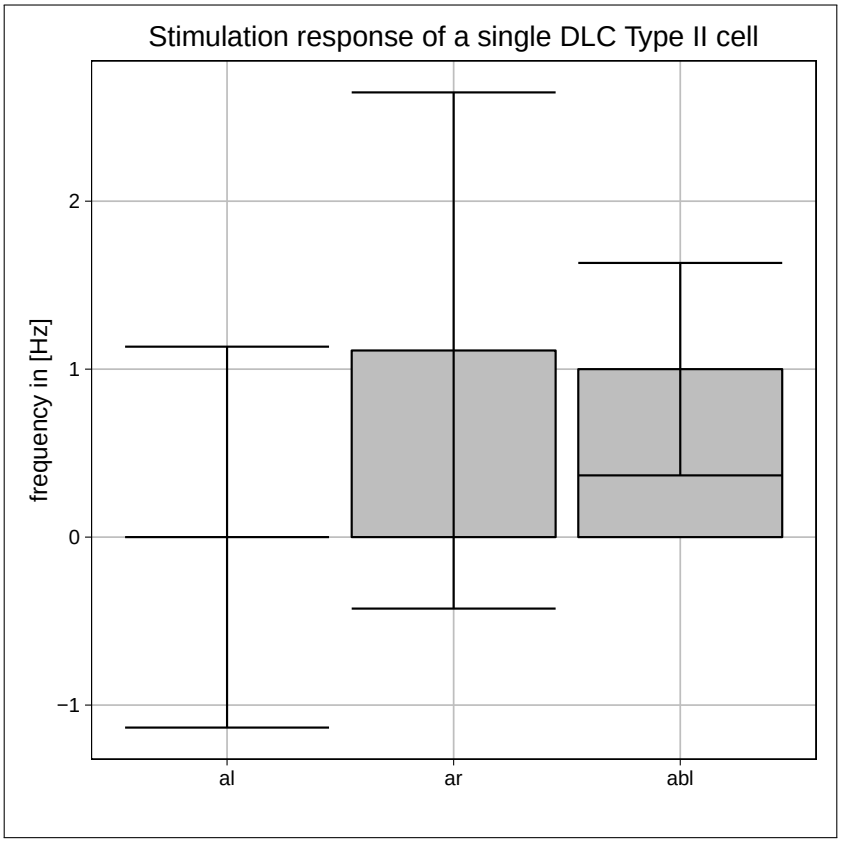

Figure 3.12: Response to stimulation of a single DLC Type II cell. Bars represent the mean frequency net difference between one second trial and one second pre-trial time in a trial block. Error bars represent a standard deviation of the mean net difference frequency for each trial block. Left side is the ipsilateral side of the body in relation to the location of the cell body in the brain, right side is the contralateral side of the body. Abbreviations: AL – antenna left (6 trials), AR – antenna right (9 trials), AB – abdomen (6 trials)

time. It is possible that only input from one side is responsible for the net increase in spike frequency.

Stimulation of antennae (fig: 3.13:A) resulted in no net increase in spike frequency after stimulation of the ipsilateral antenna and in an net increase of 1.1 Hz in the contralateral antenna. (fig: 3.12:al, ar). Both show a big variance between single trials with a standard deviation of 1.1 Hz for the ipsilateral antenna and 1.5 Hz for the contralateral one. However, it is more likely, that the DLC Type II cell receives inhibitory input from both antennae and experiences a habituation after repeated trials. Tactile stimulation in the first trial completely inhibits spiking and produces inhibitory postsynaptic potentials in both ipsi- and contralateral antennae (fig: 3.13:A, B). Habituation

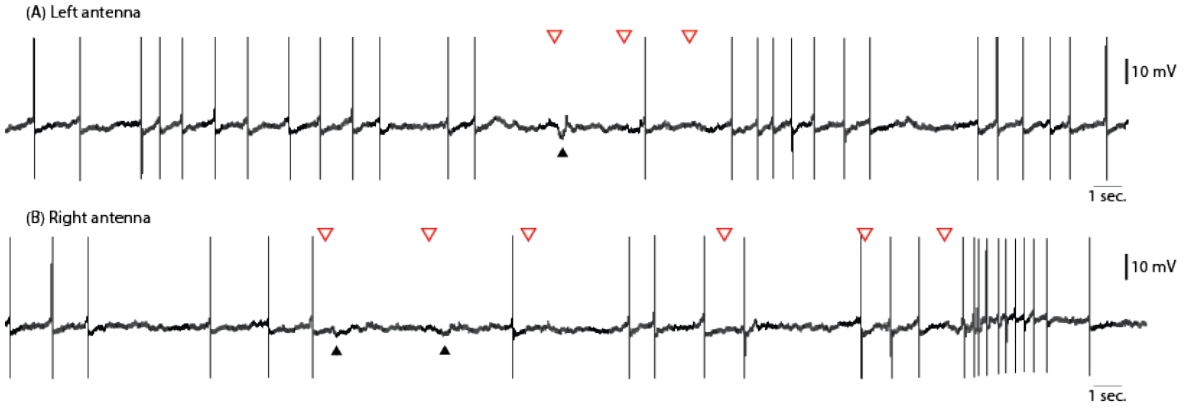

Figure 3.13: Stimulation of the DLC Type II cell. **A**: tactile stimulation of the ipsilateral (left) antenna, **B**: tactile stimulation of the contralateral (right) antenna. Red triangles represent the stimulation trigger, black triangles indicate the occurrence of inhibitory postsynaptic potentials (EPSP).

can be observed on both sides of the body with subsequent trials on each antenna being less and less inhibitive in preventing the cell from spiking. In stimulation of the right antenna trials 4-6 seem to produce no or little inhibition.

Summing up, the DLC Type receives excitatory mechanosensory input from the abdomen and inhibitory mechanosensory input from both ipsi- and contralateral antennae.

3.3.3 DLC Type III

Neuroanatomy

The DLC Type III cell has a cell body located in the dorsolateral region of the deutocerebrum in the brain(fig: 3.14.a), with an oval-shaped form, slightly rotated on the anteroposterior axis. The soma has a diameter of 40.7 μm and 28.6 μm on the major and minor axes respectively. It forms one axon which projects into the median part of the deutocerebrum and forms a junction with two branches, big in diameter (fig: 3.14.a:II, III)), one axon descending to suboesophageal ganglion (fig: 3.14.a:desc.) and one branch smaller in diameter formed from the descending axon in close proximity to the junction (fig: 3.14.a:I).

Branch I projects dorsally in the median deutocerebrum where it makes a turn and projects further in posterior direction in median tritocerebrum with little arborization.

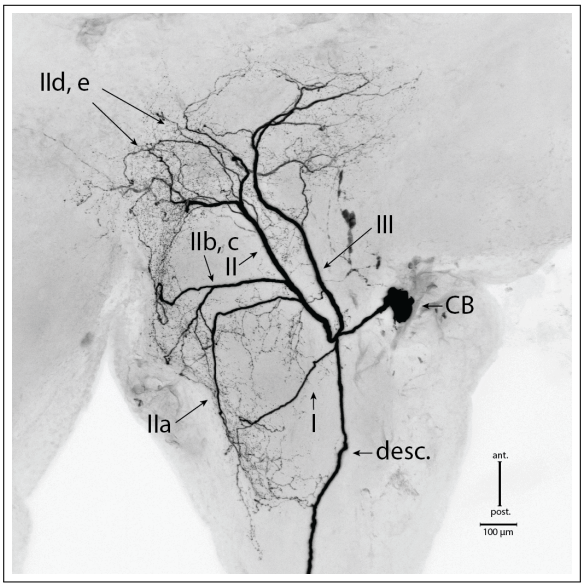

(a) Brain 20x magnification in transverse projection

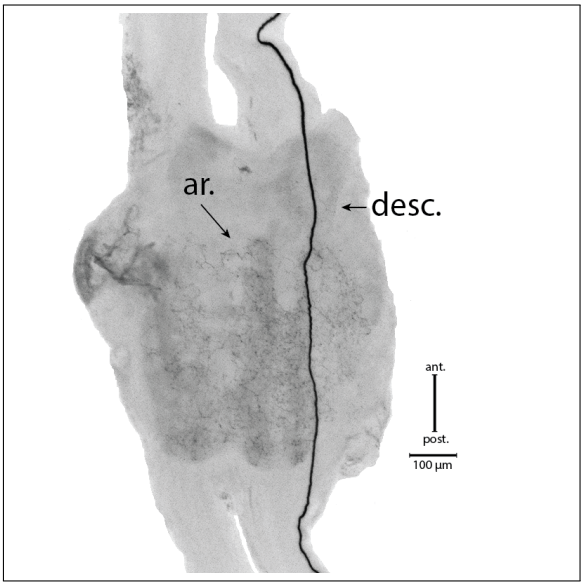

(b) SOG 10x magnification in transverse projection

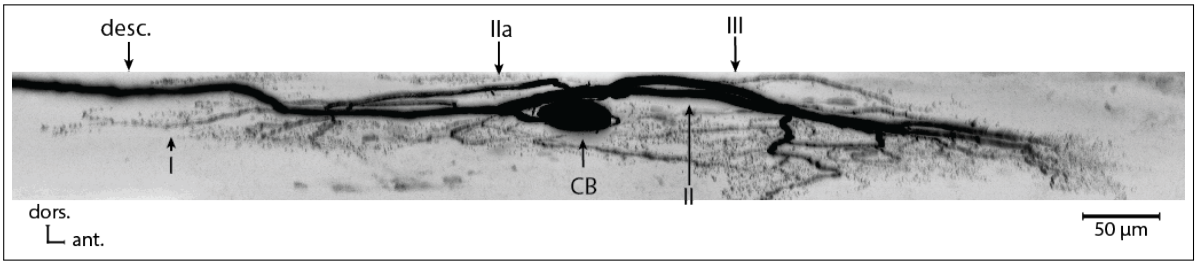

(c) Brain 20x magnification in sagittal projection

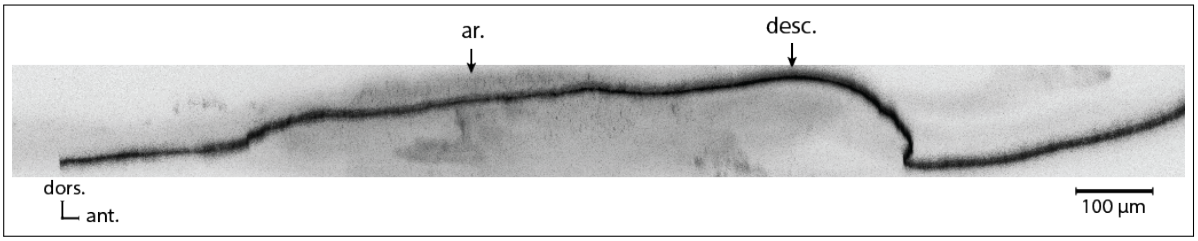

(d) SOG 10x magnification in sagittal projection

Figure 3.14: Projections of an intracellularly stained DLC Type III cell in the brain and suboesophageal ganglion. **(a)** Brain in transverse projection, **(b)** suboesophageal ganglion in transverse projection, **(c)** brain in sagittal projection, **(d)** suboesophageal ganglion in sagittal projection. Projections in the suboesophageal ganglion are probably not stained entirely. Abbreviations: I - III are secondary branches in the brain, "desc." – descending axon, CB – cell body, ant. – anterior, post. – posterior, dors. – dorsal, ar. – arborization.

Branch II ascends dorsally approximately to the direction of the central complex (CC) forming several tertiary branches with extensive arborizations which are mostly running in ventral direction (fig: 3.14.c). Branch IIa projects to the median deutocerebrum, forming finer arborizations and descending to the median tritocerebrum beneath the projection region of the branch I. Branches IIb, c project as one branch dorsally to the median deutocerebrum where they form a junction. Branch IIb forms several smaller branches all of them arborizing in the deutocerebrum. Branch IIc descends in ventral direction in a half-open loop and projects to the protocerebrum approximately to the direction of central complex. Branches IId, e project in the region of the lateral accessory lobe (LAL) and the central complex in the protocerebrum where they descend ventrally and form extensive arborizations.

Branch III projects anteriorly to the protocerebrum, mostly parallel to branch II but arborizes more lateral compared to it, approximately in the region of peduncle of the mushroom body and descending ventrally (fig. 3.14.c:III).

In suboesophageal ganglion (SOG) the axon enters on the ipsilateral side with respect to the position of the cell body in the brain. It projects through the ganglion forming several small arborizations and leaves the ganglion on the ipsilateral side (fig: 3.14.b). The axon enters the ganglion close the dorsal side and descends slightly in ventral direction inside the dorsal intermediate tract (DIT) on its way to the posterior part of the SOG (fig: 3.14.d) showing arborizations in the dorsal median and lateral parts of the ganglion, mostly in the maxillary and labial neuromeres (Tyrer and Gregory, 1982). However, not all fine projections may have been revealed.

Electrophysiology

The cell was aimed at the location of the cell body in the dorsolateral cluster, thus the recordings occurred most likely between the cell body and the junction. Cell of this type was recorded only once. No sensory stimulation was performed on this cell, since it was recorded in a nerve cord, which was dissected out ("isolated").

A spike shape overdraw (fig: 3.15.a) of a DLC Type III cell was done using 10 successive spikes. The resting potential is around -45 mV with a spike initiation threshold of -42 mV.

Spikes have a median duration of 5.5 ms (mean = 5.5 ms, standard deviation = 0.13

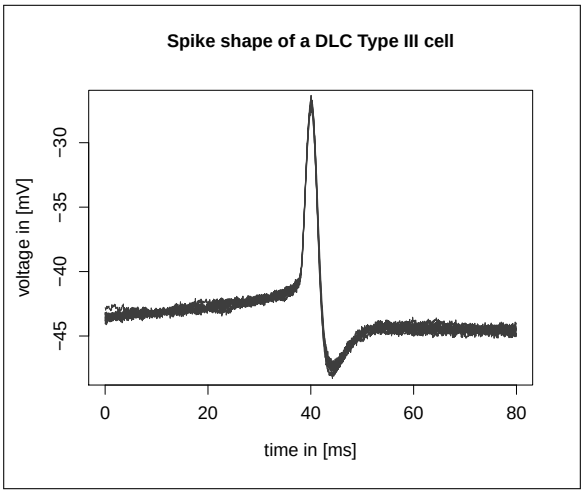

(a) Spike shape

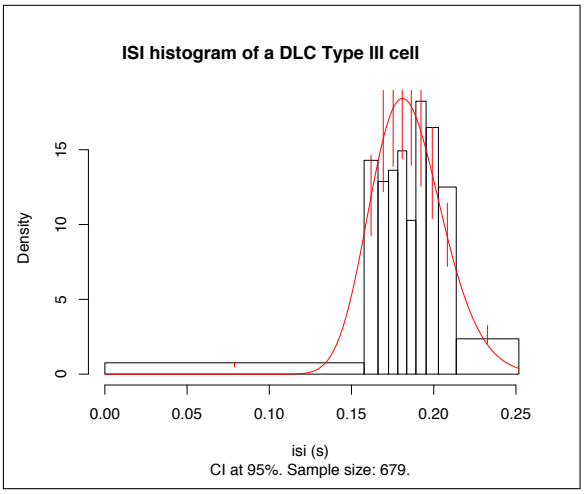

(b) Distribution of interspike invervalls

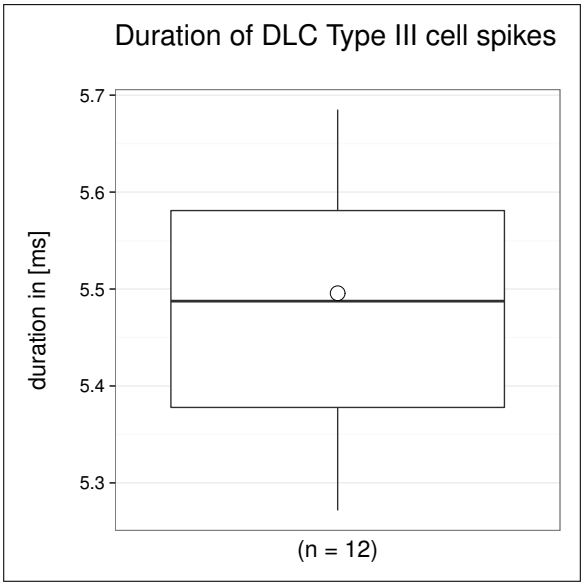

(c) Duration

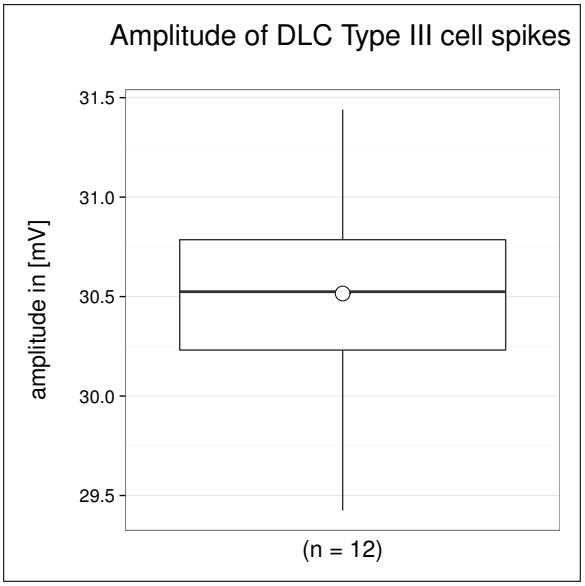

(d) Amplitude

Figure 3.15: (a) A spike shape overdraw a dorsolateral cluster (DLC) Type III cell. 10 successive spikes were used to draw a shape. **(b)** Interspike interval histogram of an DLC Type III cell. Bin width was optimised using an fitted inverse gaussian probability distribution (red line) with variable bin width, so that 10% of the interspike interval fall into each bin. Red bars represent the 95% confidence interval (CI). **(c)** Cumulative duration of 12 successive spikes, plotted as a boxplot. In boxplot, box represents the first and third quantiles, line in the middle of the box shows the median, white point stands for mean. Line represents the median (5.49 ms), dot represents the mean (5.5 ms). Standard deviation (SD) = 0.13 ms. **(d)** Cumulative amplitude of 12 successive spikes, plotted as a boxplot. Line represents the median (30.52 mV), dot represents the mean (30.52 mV). SD = 0.52 mV.

ms) as calculated from 12 successive spikes (fig: 3.15.c). The amplitude, measured from the onset of a spike to the most negative value of the hyperpolarization has a median of 30.5 mV (mean = 30.5 mV, standard deviation = 0.5 mV, n = 12) (fig: 3.15.d) with a most negative value of -49 mV and most positive value of -19.7 mV.

The cell shows a slow and monotone spiking pattern most likely due to absence of sensory input. The mean ISI is 0.185 s (5.4 Hz) with a standard deviation of 0.022 s (fig: 3.15.b) with a shortest interval of 0.133 s (7.5 Hz) and the longest interval of 0.252 s (4 Hz).

3.3.4 DLC Type IV

Neuroanatomy

The anatomy of the deutocerebral cell DLC Type IV (fig: 3.16) is similar to the anatomy of other cells in the dorsolateral cluster (DLC) cells with some distinctions. The cell body is located dorsally in the deutocerebrum, but more anterior and median than in DLC cells I - III and V. It has an oval shape, stretched on the dorsoventral axis with a size of 41.2 and 30.2 μm on the major and minor axes respectively. The axon of the cell body projects in contralateral direction and forms a junction. One branch descends in posterior direction towards SOG and thoracic ganglia, another projects in anterior brain regions. Several secondary branches split off the ascending branch and the junction between the ascending branch and the descending axon. The first branch (fig: 3.16.a:I) runs in direction of the lateral accessory lobe (LAL), turns laterally and projects with finer branches to the lateral deutocerebrum over and underneath the cell body. It forms a smaller branch Ia which projects dorsally to the median deutocerebrum. Another branch, springing off the main anterior projecting branch Ma projects to the same region in the deutocerebrum, located dorsally with respect to the Ia branch.

Several additional cell bodies were stained in the dorsolateral cluster and the lateral part of the protocerebrum. One of them is located more dorsal in relation to the axon of the DLC Type IV cell and is, most likely, co-stained over the branch II.

The second branch (fig: 3.16.a:II) splits at the junction, projects ventrally to the median tritocerebrum and then anteriorly through the median deutocerebrum to the central complex in the protocerebrum, where it forms a junction with finer branches, which project either to the ipsi- and contralateral ventral parts of fan-shaped body and

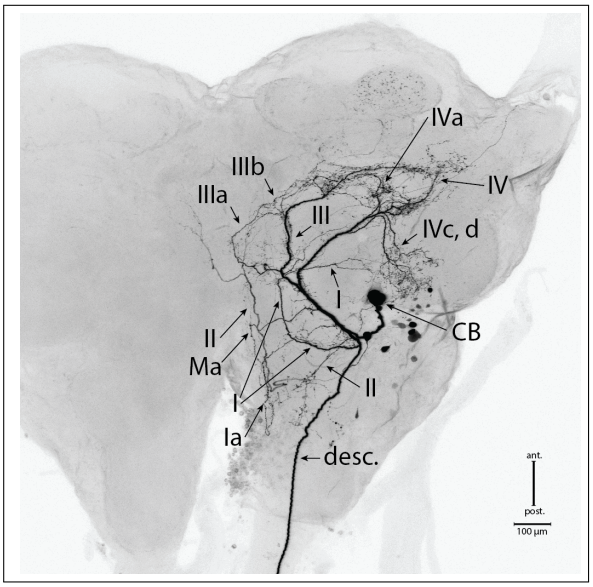

(a) Brain 10x magnification in transverse projection

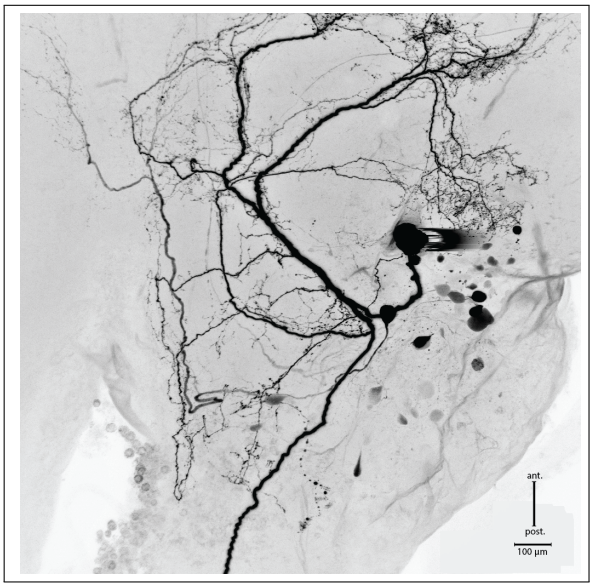

(b) Brain 20x magnification in transverse projection

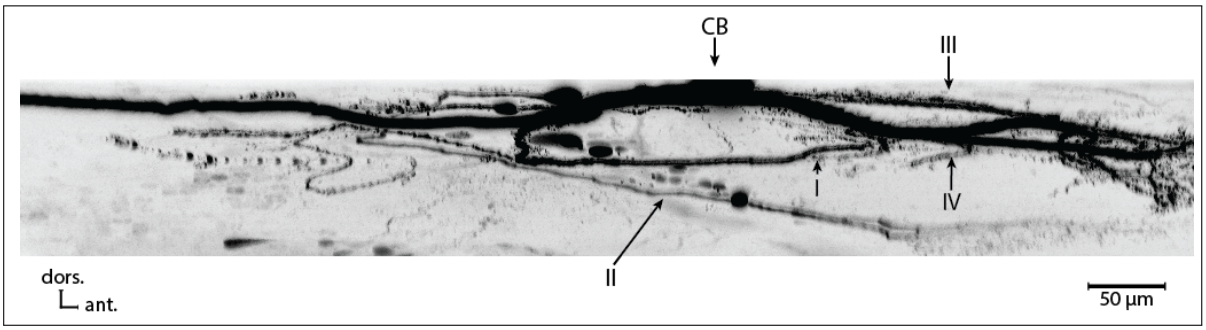

(c) Brain 20x in sagittal projection

Figure 3.16: Projections of an intracellularly stained DLC Type IV cell in the brain. Several additional cell bodies are stained in the dorsolateral cluster and lateral protocerebrum. **(a)**, **(b)** Brain transversal projection, **(c)** brain in sagittal projection. Abbreviations: I - IV and Ma are secondary branches in the brain, "desc." – descending axon, CB – cell body, Ma – main anterior branch, ar. – arborization, ant. – anterior, post. - posterior.

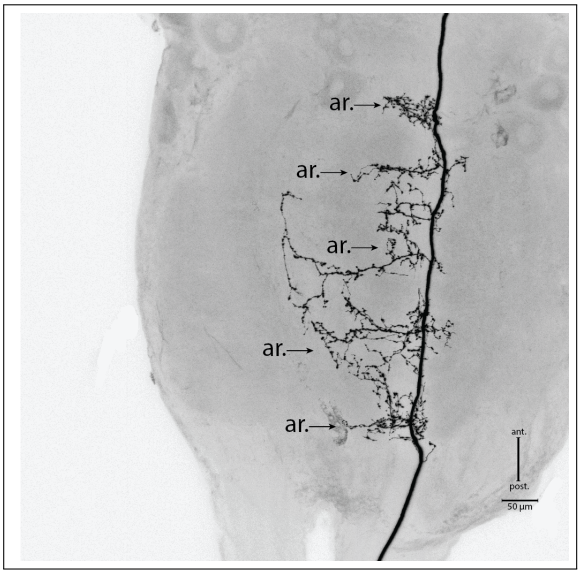

(a) SOG 20x magnification in transverse projection

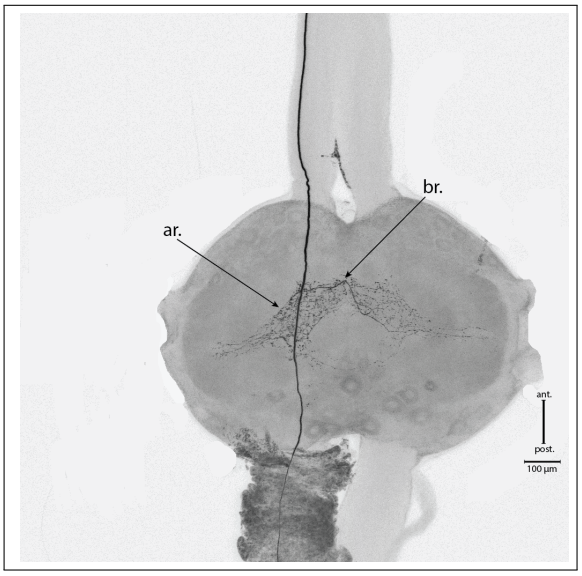

(b) prothoracic ganglion 10x magnification in transverse projection

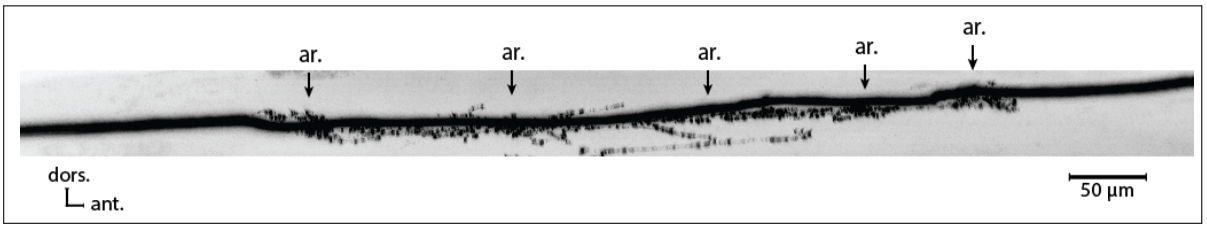

(c) SOG 20x in sagittal projection

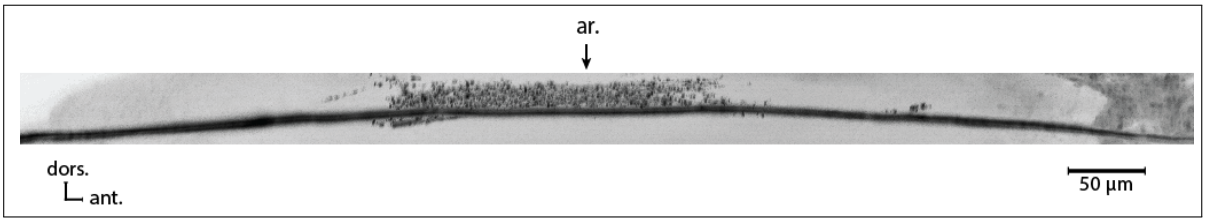

(d) prothoracic ganglion 20x in sagittal projection

Figure 3.17: Projections of an intracellularly stained DLC Type IV neurone in the suboesophageal and prothoracic ganglia. **(a)** Suboesophageal ganglion in transverse projection, **(b)** prothoracic ganglion in transverse projection, **(c)** suboesophageal ganglion in sagittal projection, **(d)** prothoracic ganglion in sagittal projection. Abbreviations: ar. – arborization, br. – branch, ant. – anterior, post. – posterior, dors. – dorsal.

the protocerebral bridge.

The third branch (fig: 3.16.a:III) consists of one branch with a bigger and two with a smaller diameter, with arborizations near the later accessory lobe in protocerebrum (IIIa, IIIb), dorsal in relation to the brach II. Branch IIIa projects into the central complex. Branch IIIb has a more complex fan-shaped projection pattern. Its median part innervates the central complex, its more lateral branches project to the peduncle of the mushroom body. It overlaps partially with the projections of the branch III, however branch III projects laterally and in ventral direction beyond the peduncle of the mushroom body.

Branch (fig: 3.16.a:IV) is consisting of one main and three secondary (IVa-c) branches. All of them are descending ventrally. Branch IVa projects within the lateral protocerebrum and into the peduncle of the mushroom body and laterally, most likely into the upper unit of the anterior optic tubercle (Homberg et al., 2003). Branch IV projects more laterally into the area of the anterior optical tract. Branches IVc, d run parallel to the deutocerebrum and arborize near the cell body and the projection area of the branch I.

In the suboesophageal ganglion the axon lies within the ispilateral dorsal intermediate tract (DIT) and projects contralaterally to the median part (fig: 3.17.a) . Inside the DIT the axon descends slightly over the length of the ganglion (fig: 3.17.c). The projections consist of at least five branches (marked with "ar.") and innervate all three neuromeres of the suboesophageal ganglion: mandibular, maxillary and the labial, according to their position. Judging on the position on the dorsoventral axis, it could project to Md DC III, V in mandibular neuromere, Mx DC I, III, VI in maxillary neuromere and Lb DC III, IV, VI, Lb SMC in the labial neuromere (Tyrer and Gregory, 1982). The most middle projection reaches far beyond the commissures and could reach the contralateral DIT.

In the prothoracic ganglion the axon lies within the ipsilateral dorsal intermediate tract (DIT) where it ascends dorsally inside the tract (fig: 3.17.b, 3.17.d). It projects dorsally. On the ipsilateral side the lateral projections branches off the axon (marked with "ar."), a smaller branch (marked with "br.") projects in the contralateral direction. Projection pattern is almost circular in the medial part of the ganglion, more extensive in the anterior part than in the posterior. The anterior part projects in regions of the dorsal part of the T-tract (TT) and dorsal commissure II (DC II). Projections in the

posterior part of the ganglion arborize in a region where dorsal commissures IV and VI (DC IV, VI) are located. Two lateral projections spring off the axon on the ipsilateral side and the projection branch on the contralateral side. They innervate dorsolateral areas of the ganglion in areas, where groups of fibres of the 4th and 3rd nerves are reported (R3i, ii, R4).

Electrophysiology

The cell was aimed at the location of the cell body in the dorsolateral cluster, thus the recordings occurred most likely between the cell body and the junction. Cell of this type was recorded only once.

Spike shape was measured using 10 successive spikes (fig: 3.18.a). Spikes are highly consistent in their form, with a resting potential at -28 mV. A shift of +3 mV is sufficient to trigger an action potential.

Spikes have a median duration of 4.5 ms (mean = 4.6 ms, SD = 0.5 ms), calculated from 12 successive spikes (fig: 3.19.a). The median amplitude of 12 successive spikes is 23.12 mV with a mean of 23.01 mV and standard deviation of 0.78 mV (fig: 3.19.b). The most negative measured value in single spike was -36.32 mV and the most positive -12.18 mV.

Cell shows a minimal interspike interval (ISI) with a shortest interval of 0.009 s (111.1 Hz) an longest 0.188 s (5.3 Hz). The mean ISI is 0.072 s (13.9 Hz) with a standard deviation of 0.027 s (fig: 3.18.b).

Experiments were performed in a semi-intact animal, with open head, partially open thorax, removed mouthparts, wings and fixed legs. Stimulations were done with a paint-brush manually. The cell body of the cell recorded from is located on the left side of the body. This side in referred to as the ipsilateral side.

DLC Type IV cell shows a higher spike and burst frequency, compared to other introduced single cell recordings (fig: 3.18.b).

The experiments consisted of blocks of single repeated trials with one stimulation each. For each trial spikes were counted in a second preceding the stimulation and the second after the stimulation. The difference between those number is the net response. In case of multiple trials in a block the mean and standard deviation of then net re-

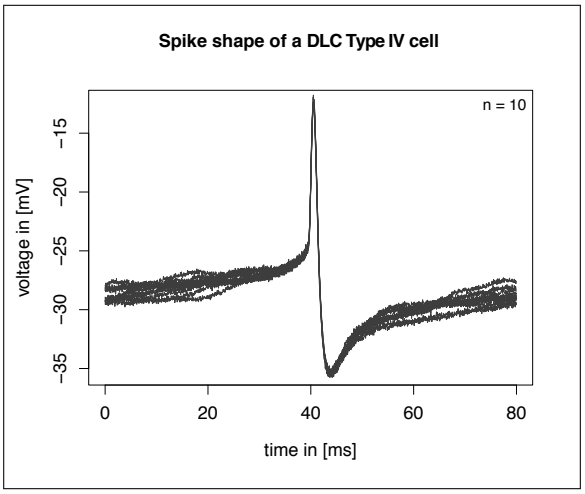

(a) Spike shape

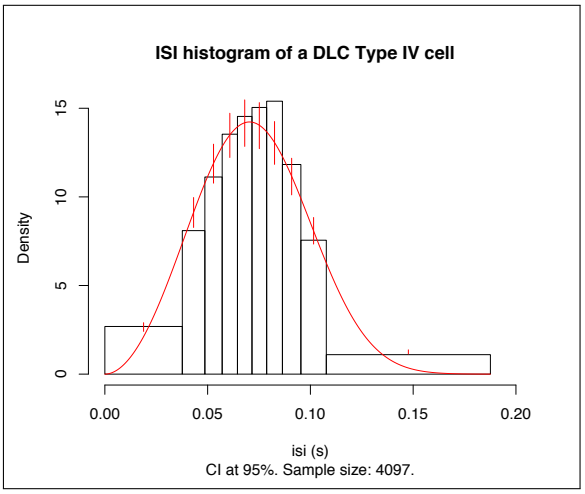

(b) Distribution of interspike intervals

Figure 3.18: (a) A spike shape overdraw of a DLC Type IV cell. 10 successive spikes were used to draw a shape. **(b)** Interspike interval histogram of a DLC Type IV cell. Bin width was optimised using an fitted Weibull probability distribution (red line) with variable bin width, so that 10% of the interspike interval fall into each bin. Red bars represent the 95% confidence interval (CI).

sponses were calculated and plotted.

Tactile stimulation of abdomen increased the spike frequency on both sides of the body, with a stronger net frequency increase (7.7 Hz) on the ipsilateral side compared to 3 Hz increase on the contralateral side (fig: 3.20:abr, abl). Frequencies are consistent between single trials resulting in small amount of deviation from the mean.

A decrease in mean net spike frequency was observed after tactile stimulation of both sides of the thorax with a higher decrease on the ipsilateral side of the body (fig: 3.20:tl, tr). However, the net decrease of frequency is lower then the spread of the mean frequency for the contralateral side of thorax and as high as the spread for the ipsilateral side which may indicate a weak inhibitory input with a rapid habituation or no input at all.

Both ipsi- and contralateral cerci were stimulated simultaneously and show no consistent effect with a small increase of net mean frequency of 1.3 Hz and standard deviation of 4.9 Hz (fig: 3.20:crc).

No difference in spike frequency (fig: 3.20:snd) can be found in response to acoustic

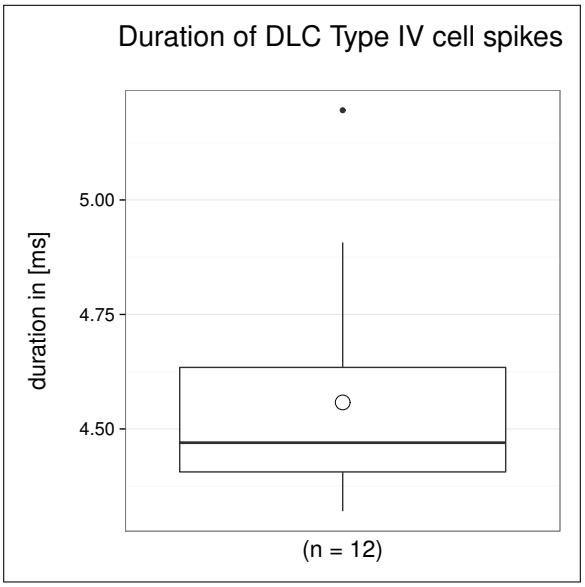

(a) Duration

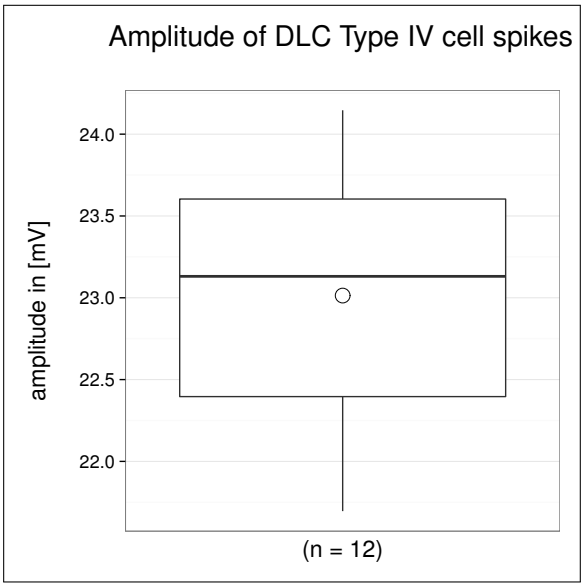

(b) Amplitude

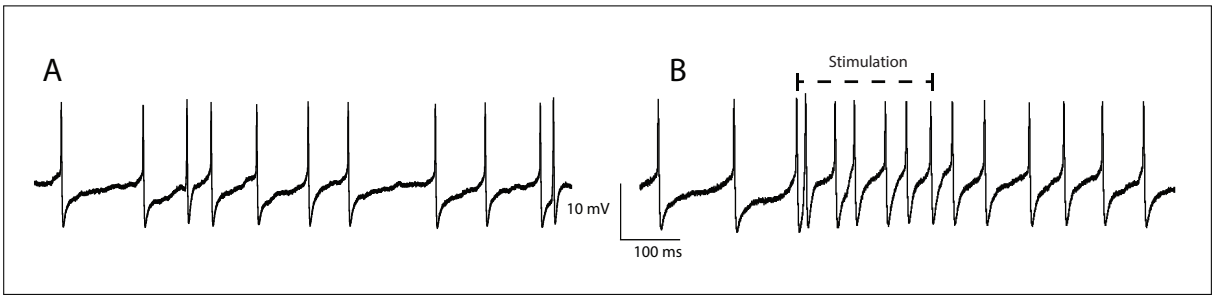

(c) Spiking pattern

Figure 3.19: Properties of a single DLC Type IV cell. **(a)** Cumulative duration of 12 successive spikes, plotted as a boxplot. In boxplot, box represents the first and third quantiles, line in the middle of the box shows the median, white point stands for mean. Line represents the median (4.6 ms), dot represents the mean (4.5 ms). Standard deviation = 0.3 ms. **(b)** Cumulative amplitude of 12 successive spikes, plotted as a boxplot. Line represents the median (23.13 mV), dot represents the mean (23.01 mV). Standard deviation = 0.8 mV. Whiskers represent the 25th and 75th percentiles. **(c)** Intracellular recordings of a DLC Type IV cell before (A) and after (B) tactile stimulus application to the ipsilateral (left) side of the abdomen.

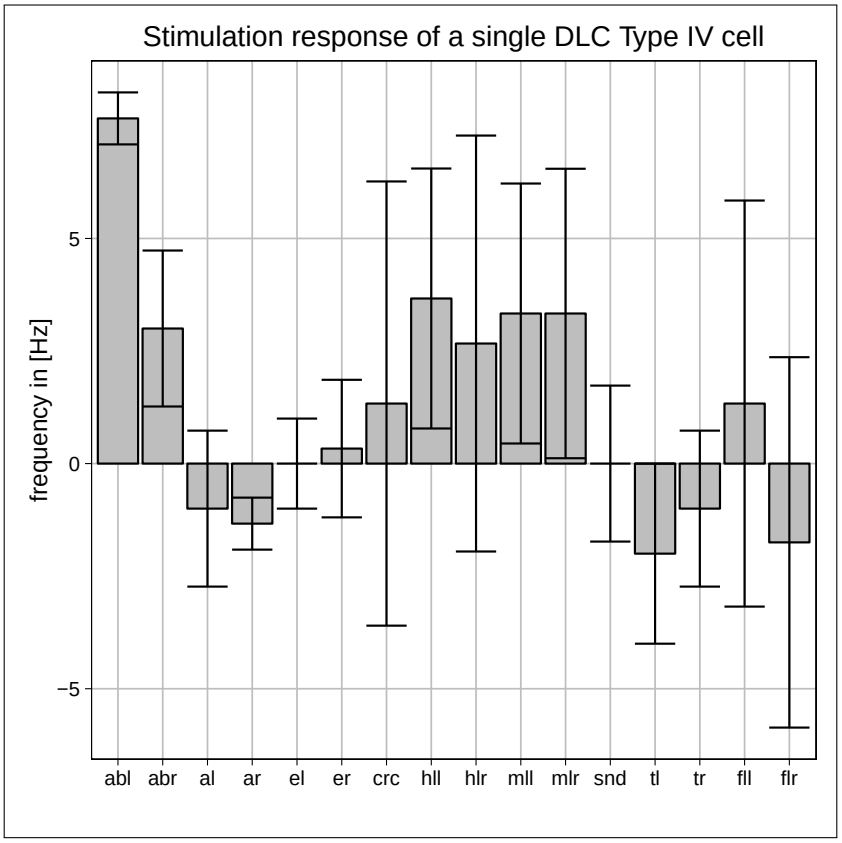

Figure 3.20: Response to stimulation of a single DLC Type IV cell. Bars represent the mean frequency net difference between one second trial and one second pre-trial time in a trial block. Error bars represent a standard deviation of the mean net difference frequency for each trial block. Left side is the ipsilateral side of the body in relation to the location of the cell body in the brain, right side is the contralateral side of the body. Abbreviations: ABL – abdomen left (3 trials), ABR – abdomen right (3 trials), AL – antenna left (3 trials), AR – antenna right (3 trials), EL – eye left (3 trials), ER – eye right (3 trials), CRC – cerci (3 trials), HLL – hind leg left (3 trials), HLR – hind leg right (3 trials), MLL – mid leg left (3 trials), MLR – mid leg right (3 trials), SND – sound (3 trials), TL – thorax left (3 trials), TR – thorax right (3 trials), FLL – front leg left (3 trials), FLR – front leg right (4 trials).

stimulation which was done by rattling a bound of metallic keys.

Tactile stimulation of antennae was performed on the ipsilateral and contralateral sides, resulting in net decrease of mean frequency on both of them (fig: 3.20:al, ar). They are similar in strength of response with a net decrease of 1.3 Hz on the contralateral side and 1 Hz on the ipsilateral side. However, the results are inconsistent between single trials for the ipsilateral antenna, resulting in high spread and indicating a weaker effect or no effect at all.

Tactile stimulation of both hind legs was followed by an net increase of mean spike frequency (fig: 3.20:hll, hlr). However, only in the ipsilateral leg the stimulation evokes a strong response with 3.6 Hz which is not overshadowed by the spread of the mean. The results for the contralateral leg are less consistent with a lower net increase in spike frequency (2.6 Hz) and high spread of 4.6 Hz. Thus, one cannot be certain about whether the DLC Type IV cell receives bilateral input from both hind legs or only from the ipsilateral one.

Stimulation of the middle pair of legs increased the spike frequency on both sides of the body(fig: 3.20:mll, mlr). The net mean response frequency of the ipsilateral leg since is most likely not due to spontaneous spiking even though it shows a relatively high amount of spread. The contralateral middle leg shows the same mean net increase in frequency of 3.3 Hz after stimulation but is slightly less consistent between single trials. It may indicate a lower strength of response or could be due to slight differences in applied pressure.

Stimulation of the frontmost pair of legs induced a slight decrease net mean spike frequency in the ipsilateral leg and a slight increase in the contralateral leg (fig: 3.20:fll, flr). However, variation between single trials is high, resulting in high spread. It suggests, that the net difference between trials and pre-trials is most likely due to spontaneous spiking.

Visual stimulation of the left and right eye with a white disk, moved in the lateral visual field of the animal shows only slight increase in frequency in the ipsilateral eye and no net increase in frequency in the contralateral eye(fig: 3.20:el, er). Both results are accompanied with a high spread. It suggest that the DLC Type IV cell receives no visual input.

Summing up, the DLC Type IV cell responds with an increase of spike frequency to mechanosensory stimulation of both sides of the abdomen, ipsilateral hind leg, both middle legs and tactile stimulation of the contralateral antenna. Due to high variation of spontaneous spike frequency the results acquired by stimulation of the contralateral hind leg and ipsilateral side of the thorax are unclear and require further investigations.

3.3.5 DLC Type V

Neuroanatomy

The cell body of the DLC Type V cell is located dorsally in the lateral deutocerebrum and is slightly stretched on the lateral axis (fig: 3.21.a:CB). It measures 47.5 μm on its major and 28.7 μm on its minor axis. The cell body forms an axon which projects in direction of the median deutocerebrum and forms a junction. One part of the junction forms an axon (fig: 3.21.a:desc.) which descends in the ipsilateral connective forming one branch (fig: 3.21.a:IV). The ascending part of the junction forms three bigger secondary branches (fig: 3.21.a:I-III) and several smaller (fig: 3.21.a:V-VI).

Branch I (fig: 3.21.a, 3.21.c:I) projects in the middle part of the brain and the antennal lobe. It forms three finer branches. One of them projects ventrally in the lower divisions of the central body and arborizes there. Another two make a turn in ipsilateral direction in relation to the cell body, descend ventrally and form fine arborization in the antennal lobe.

Branch II (fig: 3.21.a, 3.21.c:II) ascends in anterior directions forming 3 bigger branches and several smaller. Branch IIa projects to the protocerebral bridge and the upper divisions of the central body. Branches IIb and c form finer arborizations which project dorsally and above the ipsilateral peduncle of the mushroom body.

Branch III arborizes in two bigger branches with each of them forming several smaller with a finer arborization (fig: 3.21.a, 3.21.c:III). Branch IIIa descends in ventral direction and arborizes in the region where peduncle of the mushroom body is located. Branch IIIb projects in lateral direction in the protocerebrum, forming arborizations near the lobula complex and in the dorsal part of the protocerebrum.

Branch IV (fig: 3.21.a:IV) is formed by the descending axon and projects to the median protocerebrum and further to the contralateral side of the brain with respect to the position of the cell body. It forms no notable arborizations but could be the branch which co-stained an axon and finer arborization of a cell on the other side of the brain. Judged by anatomy, it is probably the same cell.

Branches V and VI (fig: 3.21.a:V, VI) are formed from the ascending part of the axon right after the junction. Branch V descends in ventral direction within the deutocerebrum and projects, together with finer arborizations of the branch I, to the antennal

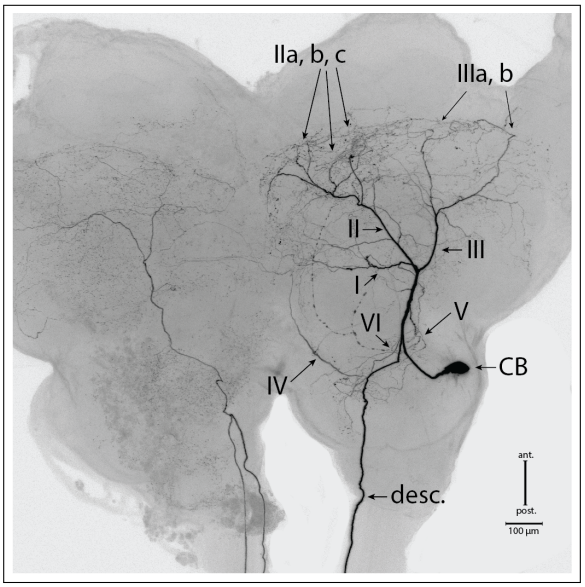

(a) Brain 20x magnification in transverse projection

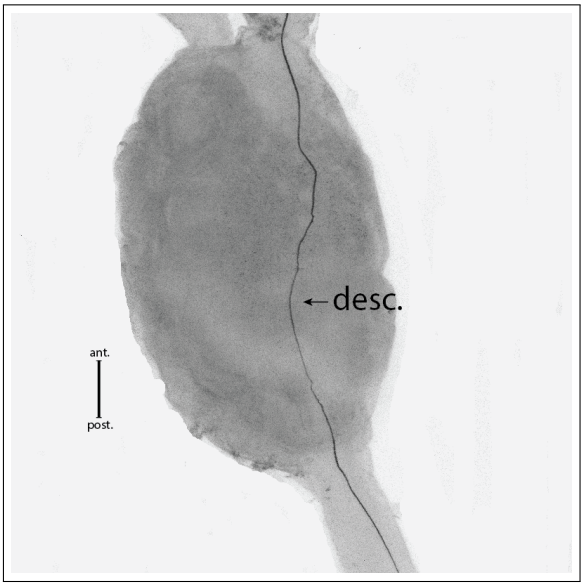

(b) SOG 10x magnification in transverse projection

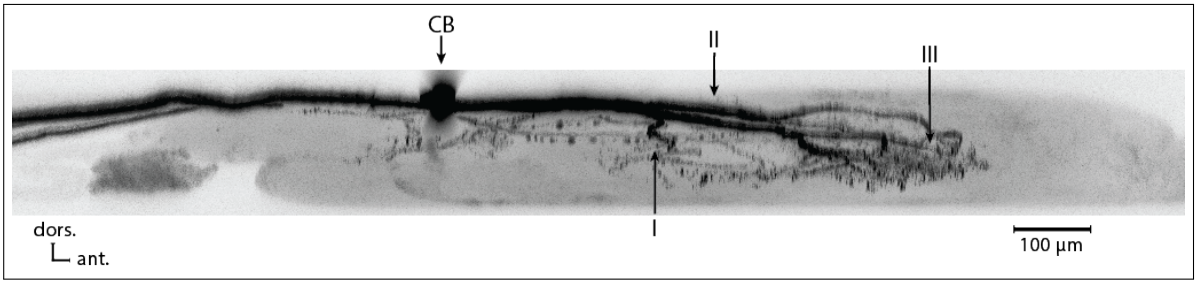

(c) Brain 10x magnification in sagittal projection

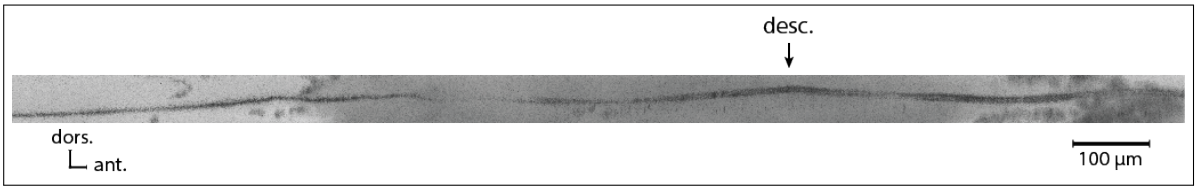

(d) SOG 10x magnification in sagittal projection

Figure 3.21: Projections of an intracellularly stained DLC Type V cell in the brain and suboesophageal ganglion. **(a)** Brain in transverse projection, **(b)** suboesophageal ganglion in transverse projection, **(c)** brain in sagittal projection. **(d)** suboesophageal ganglion in sagittal projection. Projections of another, probably the same, cell are co-stained on the left side in **(a)**. Abbreviations: I - VI are secondary branches in the brain, "desc." – descending axon, CB – cell body, ant. – anterior, post. – posterior, dors. – dorsal.

lobe. Branch VI stays dorsal and forms finer arborizations in the median part of the deutocerebrum.

In the suboesophageal ganglion the axon enters the ganglion on the ipsilateral side of the ganglion with respect to the cell body and descends without any notable arborizations (fig: 3.21.b). However, the latter may be due to a poor staining in the suboesophageal ganglion in general. The axon projects with the dorsal intermediate tract (DIT) and leaves the ganglion on the ipsilateral side through the connective. It descends slightly in ventral direction within the DIT (fig: 3.21.d).

Electrophysiology

The cell was aimed at the location of the cell body in the dorsolateral cluster, thus the recordings occurred most likely between the cell body and the junction. Cell of this type was recorded only once.

A spike shape overdraw was done using 10 successive spikes (fig: 3.22.a). The spikes are characterised through the large overshooting potential and prolonged period of hyperpolarization with a resting potential around -60 mV and a spike initiation threshold of -55 mV.

The duration of a single spike (fig: 3.22.c), measured from the onset to the most negative point of the hyperpolarization, has a median of 4.8 ms (mean = 4.73, SD = 0.16 ms, n = 12). The amplitude of a single spike(fig: 3.22.d) has a median of 65.29 mV (mean = 65.22 mV, SD = 0.47 mV, n = 12), with -16.79 mV as the most positive and -82.87 mV as the most negative potential.

The cell exhibits a slow frequency spiking pattern with an interspike interval (ISI) between 0.029 sec (34.5 Hz) as the shortest ISI and 2.205 sec (0.45 Hz) as the longest ISI (fig: 3.22.b). This includes times where the cell was stimulated. The mean ISI is 0.412 sec and its standard deviation is 0.269 sec, which is equivalent to an average spike frequency of 2.43 Hz.

Experiments were performed in a semi-intact animal, with open head, partially open thorax, removed mouthparts, wings and fixed legs. Stimulations were done with a paintbrush manually. The cell body of the cell recorded from is located on the left side of the body. This side in referred to as the ipsilateral side.

The experiments consisted of blocks of single repeated trials with one stimulation each. For each trial spikes were counted in a second preceding the stimulation and the second after the stimulation. The difference between those number is the net response.

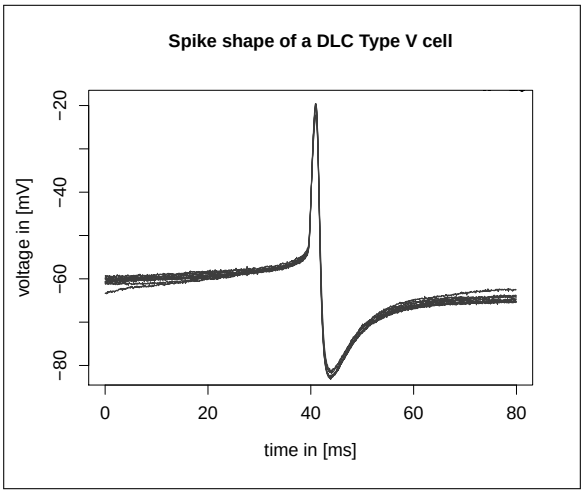

(a) Spike shape

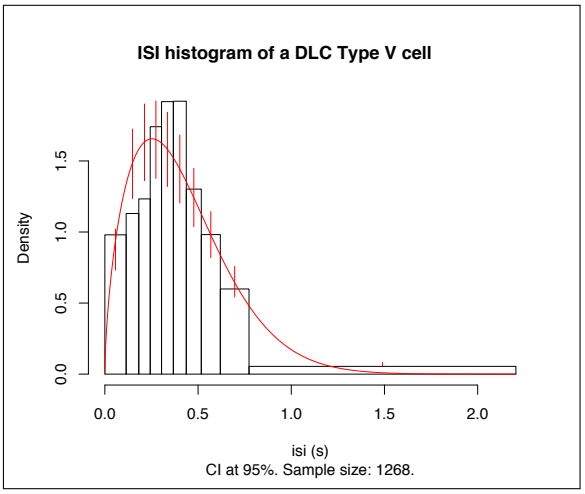

(b) Distribution of interspike intervalls

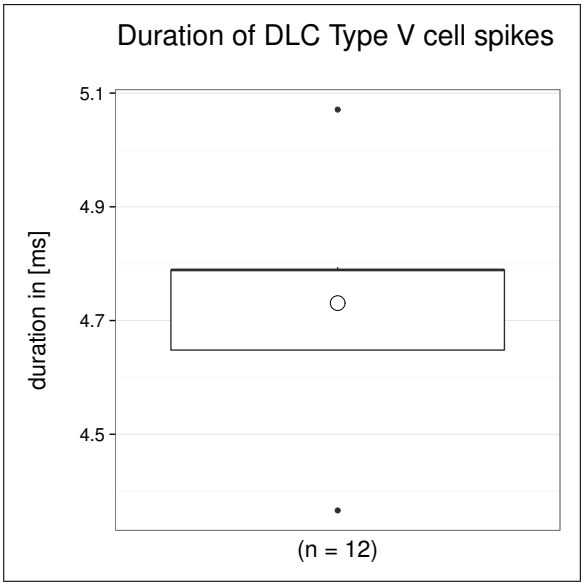

(c) Duration

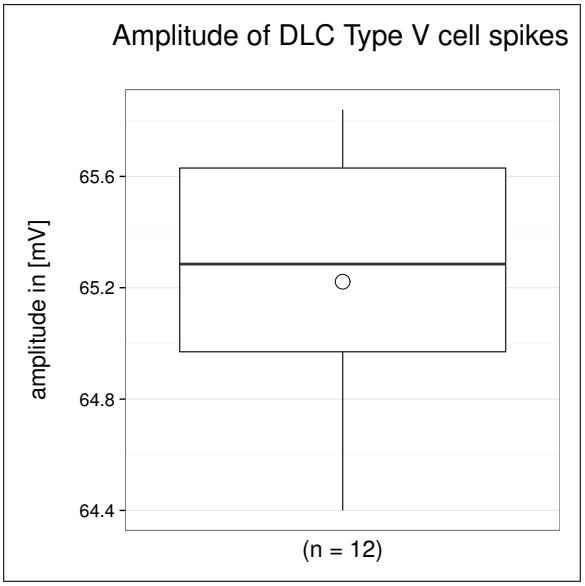

(d) Amplitude

Figure 3.22: (a) A spike shape overdraw of a DLC Type V cell. 10 successive spikes were used to draw a shape. **(b)** Interspike interval histogram of an DLC Type V cell. Bin width was optimised using an fitted weibull probability distribution (red line) with variable bin width, so that 10% of the interspike interval fall into each bin. Red bars represent the 95% confidence interval (CI). **(c)** Cumulative duration of 12 successive spikes, plotted as a boxplot. In boxplot, box represents the first and third quantiles, line in the middle of the box shows the median, white point stands for mean. Line represents the median (4.8 ms), dot represents the mean (4.73 ms). Standard deviation = 0.16 ms. **(d)** Cumulative amplitude of 12 successive spikes, plotted as a boxplot. Line represents the median (65.29 mV), dot represents the mean (65.22 mV). SD = 0.47 mV.

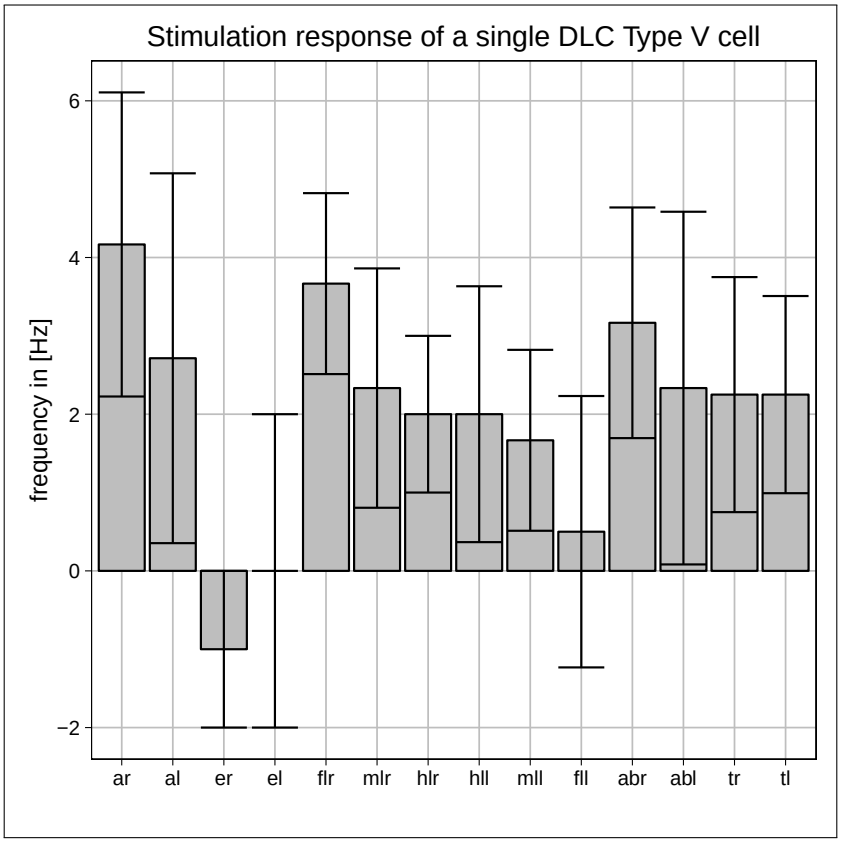

Figure 3.23: Response to stimulation of a single DLC Type V cell. Bars represent the mean frequency net difference between one second trial and one second pre-trial time in a trial block. Error bars represent a standard deviation of the mean net difference frequency for each trial block. Left side is the ipsilateral side of the body in relation to the location of the cell body in the brain, right side is the contralateral side of the body. Abbreviations: ABL – abdomen left (6 trials), ABR – abdomen right (6 trials), AL – antenna left (9 trials), AR – antenna right (9 trials), EL – eye left (3 trials), ER – eye right (3 trials), HLL – hind leg left (4 trials), HLR – hind leg right (3 trials), MLL – mid leg left (3 trials), MLR – mid leg right (3 trials), SND – sound (trials), TL – thorax left (4 trials), TR – thorax right (4 trials), FLL – front leg left (4 trials), FLR – front leg right (3 trials).

In case of multiple trials in a block the mean and standard deviation of then net responses were calculated and plotted.

Tactile stimulation of both ipsi- and contralateral sides of the abdomen increased the spike frequency on both sides. (fig: 3.23:abl, abr). However the contralateral side (right) shows a stronger net increase in frequency (3.2 Hz) compared to the ipsilateral side of the abdomen (2.3 Hz). The ipsilateral side shows a spread which is almost as high as the net increase suggesting a weak input or a high variation between trials.

Tactile stimulation of the thorax increased the net spike frequency on both sides to 2.25 Hz compared to the pre-trial, with the contralateral sides of the thorax showing a slightly higher deviation between single trials (fig: 3.23:tl, tr).

Both ipsi- and contralateral antennae show an net increase in frequency after tactile stimulation (fig: 3.23:al, ar). The contralateral antenna shows a higher net increase in frequency (4.17 Hz) compared to the ipsilateral (2.7 Hz) which has a high deviation additionally.

Tactile stimulation of both hind legs increase the net frequency to 2 Hz on both ipsi- and contralateral leg compared to the pre-trial (fig: 3.23:hll, hlr). However, the ipsilateral (left) leg shows a higher spread between single trials.

Both middle legs increase the net spike frequency compared to the pre-trial after a tactile stimulation (fig: 3.23:mll, mlr). The contralateral middle leg shows a higher net increase with 2.3 Hz compared to the ipsilateral middle leg with 1.7 Hz.

Tactile stimulation of both front legs increased the net frequency in the contralateral (right) leg to 3.6 Hz (fig: 3.23:flr). Small net increase combined with a big spread can be observer after the stimulation of the ipsilateral leg, suggesting no effect (fig: 3.23:fll).

Visual stimulation was done with a white disk, moved in the lateral visual field of the animal. It shows no net increase and hight spread after stimulation of the ipsilateral eye (fig: 3.23:el). Stimulation of the contralateral shows an decrease in spike frequency of 1 Hz compared to the pre-trial (fig: 3.23:er). However, the spread between trials is high as the net decrease in frequency.

Summing up, the DLC Type V cells increases the spike frequency after both ipsi- and contralateral stimulation of antennae, thorax, abdomen and both hind and middle legs. The cells seems to receive excitatory input only from the contralateral front leg. Additionally, the contralateral eye may receive a weak inhibitory input, however it is not clear what kind. It may be related to a specific kind or movement in specific direction in the visual field of the animal and remains a subject to further investigations. The DLC Type V cells seems to have a stronger input from the contralateral side of the body resulting either in a higher net increase of frequency or a smaller spread. However this may be due to manual stimulation and differences in applied pressure.

3.3.6 Summary of properties of DLC Type I-V cells

Cells, introduced in (3.3) show similarities in morphology, spike properties and response to stimulation.

All cells, introduced in (3.3) have a cell body in the DLC, an axon descending in the nerve cord and a characteristic position of the axon in the suboesophageal ganglion. Additionally, cells, stained in the prothoracic ganglion (DLC Type I and IV) show a similar type of arborization. In the brain, those cells project to the regions of the lateral accessory lobe, central complex, the peduncle of the mushroom body in the protocerebrum and the median deutocerebrum.

DLC Type I-V cells show a spike shape with an overshooting hyperpolarization (figs. 3.6.a, 3.11.a, 3.15.a, 3.18.a and 3.22.a) and slow spike frequencies with a maximum of 13.9 Hz in DLC Type IV cell and a minimum of 0.79 Hz in DLC Type II cell (table: 3.1). Additionally, DLC Type I, II, IV and V cells receive excitatory mechanosensory input from the abdomen.

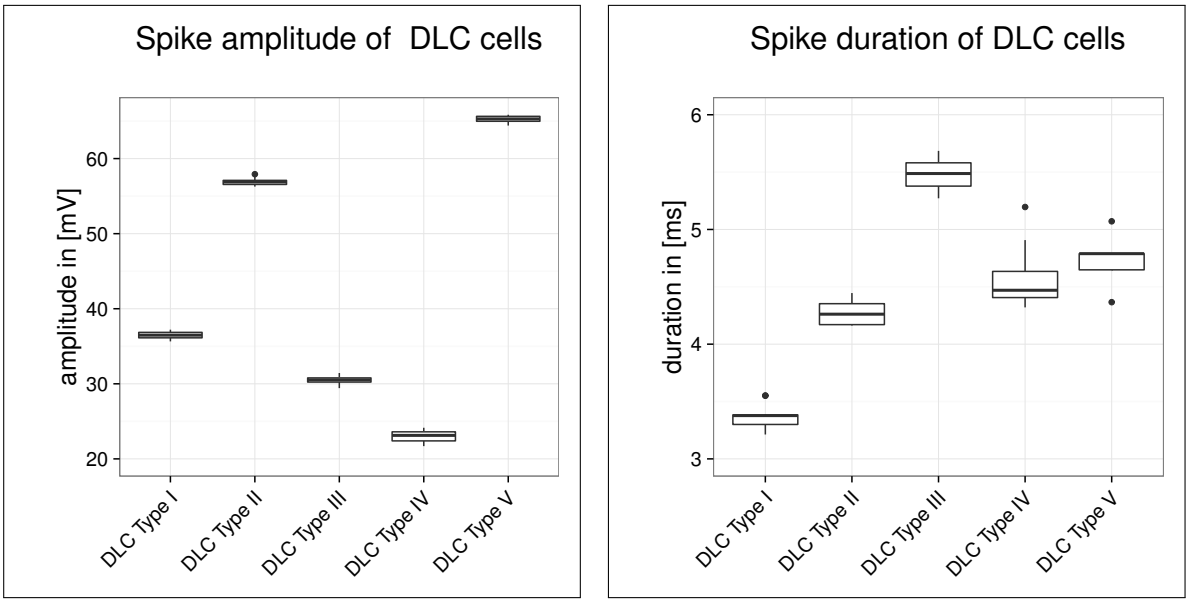

(a) Spike amplitude

(b) Spike amplitude

Figure 3.24: (a) Spike amplitude of DLC Type I-V cells, calculated from 12 spikes for each cell. **(b)** Spike duration of DLC Type I-V cells, calculated from 12 spikes for each cell. In boxplot, box represents the first and third quantiles, line in the middle of the box shows the median.

Cell type	Amplitude [mV]	Duration [ms]	Frequency [Hz]	Resting potential [mV]
DLC Type I	36.6	3.36	5.3	-50
DLC Type II	56.83	4.28	0.79	-48
DLC Type III	31	5.5	5.4	-45
DLC Type IV	23.12	4.5	13.9	-28
DLC Type V	65.29	4.8	2.43	-60

Table 3.1: Comparison of spike properties between cells. For amplitude, duration and frequency mean values were used.

4 Discussion

The main goal of this work was to provide a better insight into the morphology and function of descending cells in the dorsolateral cluster of the locust *Schistocerca gregaria*. Additionally, general morphology and the size of cells in the cluster should be evaluated.

4.1 General morphology of the dorsolateral cluster

The dorsolateral cluster (DLC) in the brain of *Schistocerca gregaria* consists of approximately 200 cells, as was shown by counting cells in HRP preparations. However, most of them have a small sized cell body with only few cells having a cell body with a size of more than 40 μm. Some cells in the DLC were found to descend further then suboesophageal ganglion. In retrograde stainings between 4. and 5. abdominal ganglia, done in this study, only up to four descending cells were stained. In stainings, made between the suboesophageal and prothoracic ganglia, five cells with a descending axon were stained in the dorsolateral cluster (Laboratory of Prof. Dr. H.-J. Pflüger, unpublished results). Despite some minor discrepancies in measured cell sizes between anti-HRP and retrograde stainings with neurobiotin, most likely due to different cytochemical protocols and different amount of tissue shrinkage, these descending cells are among the biggest cells in the DLC with a size of 40 and 42 μm. These values are in accordance with the values reported by Kononenko et al. (2009), where a cell diameter of 40-60 μm was mentioned for octopaminergic cells in the dorsolateral part of the brain (OA3/TA).

Cell bodies of these cells are positioned close to each other in the DLC, as was shown in retrograde stainings (3.1). It was proposed by Goodman et al. (1980) that cells, originating from the same neuroblast and having the same birth position in the timeline, share similar features, including morphology, neurotransmitter and electrical properties. These findings were supported in later studies on DUM-cells in thoracic ganglia of the locust (Taghert and Goodman, 1984; Thompson and Siegler, 1993; Jia and Siegler, 2002). Moreover, there are indications that cells sharing the same neuroblast and simi-

lar birth place tend to share a similar spatial location in the brain (Boyan et al., 2010). This findings could explain the morphological similarities between cells introduced in single cell recordings.

4.2 Methods used in this study

Anti-octopamine/anti-tyramine immunocytochemical stainings, combined with retrograde stainings with neurobiotin showed some problems regarding immunoreactivity of the anti-octopamine. Cells in the DLC were not stained at all (in 3 out of 5 preparations), or only on the side contralateral to the DLC cluster, where descending cells were stained with neurobiotin. There is also a discrepancy between the number of stained octopaminergic cells in the DLC cluster on different sides of the same preparation. It appears that cells already stained with neurobiotin are less like to express anti-octopamine immunoreactivity. This makes exact conclusions about which of the descending cells are octopaminergic difficult, since they can be correlated only about their size.

The immunocytochemical stainings with anti-tyramine/anti-octopamine were not controlled for the sex of animal. However, it is unlikely that sex specific differences are the cause for different number of cells stained with anti-octopamine antibodies in the brain, since such sexual dimorphism in octopaminergic cells was found to affect only projection patterns of octopaminergic cells in the genital ganglia, not their number (Stevenson et al., 1994).

Anti-HRP stainings provide a good insight into the general anatomy of the DLC. They should be scanned in a high resolution, though, since the DLC consists mostly of small cells which are not recognisable otherwise. In general, the anti-HRP scans showed some possible tissue shrinkage, since even the biggest cells in the cluster were smaller in preparations done with HRP stainings compared to cells measured in preparations with retrograde and anterograde stainings. This is most likely an issue of the protocol used.

Intracellular single cell recordings and stainings provide a good insight into the electric properties, general morphology of single cells and sensory input they receive, but fail short on providing a general picture about the whole cluster. In this study, different methods were combined to get an overview of the DLC and the descending cells in it.

DLC Type I-V cells, introduced in single cell recordings, are most likely, different cells, despite DLC Type I-IV cells showing some similarities in anatomy. They all have different spike amplitudes, but an amplitude is dependent on the goodness of seal between the membrane of the cell and the electrode and on exact location where the cell was recoded. The spike frequency may be dependent on the general state of arousal in the animal and is similar in DLC Type I and III cells. Additionally, the DLC Type II cell was recored in an isolated nerve cord, making a direct comparison of frequency to other cells different. However, the duration of a spike is an intrinsic cell property and is different between all DLC cells.

4.3 Octopaminergic and tyraminergic immunoreactivity of the DLC Type I-V cells

Under the four octopaminergic/tyraminergic cells in the OA3/TA cluster only two cells were found to descend to suboesophageal ganglion and further (Kononenko et al., 2009)). Another two are local to the brain and project laterally within the posterior optical tract. Since the cells, introduced in the single cell recordings and stainings are among the cells with the biggest cell body diameter, the two descending octopaminergic cells mentioned by Kononenko et al. (2009) should be among them. However, it cannot be exactly stated in this study, which of the introduced DLC Type I-V cells are octopaminergic. There are some indicators, that the two descending cells with the octopaminergic activity have to be among the DLC Type I-III or Type V cells.

The cell body of the DLC Type IV cell is located more anterior than cells of the DLC, on the edge to the posterior dorsolateral protocerebrum. Even though the position of soma can slightly vary after the immunohistochemistry and there is certainly some variability dependent on the particular animal, the DLC Type IV cell has a higher spike frequency (fig: 3.1) compared to the rest of introduced DLC cells. Additionally, cells with such anterior soma position in the cluster cannot be found on the anti-octopamine stainings and retrograde stainings from abdominal connectives, nor were such cells found in anti-octopamine/anti-tyramine stainings by Kononenko et al. (2009). Since cells with the same neurotransmitter tend to stay in close neighbourhood, the DLC Type IV cell is probably a progeny of the same neuroblast but on the different point in the timeline.

Electrical properties of the DLC Type I-III and V cells show some similarities to

efferent octopaminergic DUM cells in thoracic ganglia. All cells show a spike shape with a prominent phase of afterhyperpolarization (AHP), prolonged phase of repolarization and low spiking frequency akin to octopaminergic efferent DUM neurones in thoracic ganglia, which show similar spiking properties and slow depolarization. The DLC Type IV shows the same characteristic spike shape with a higher resting potential and higher spike frequency compared to DLC Type I-III and V cells.

In efferent octopaminergic DUM cells in the thoracic ganglia the specific spike shape and spiking properties are regulated by a number of different ionic currents and a diversity of channels. Ca^{2+}-activated currents ($I_{K,\,Ca}$ are responsible for the prominent afterhyperpolarization, transient and maintained low-voltage-activated Ca^{2+} currents ($I_{Ca,t}$, $I_{Ca,m}$) are responsible for the slow reaching of the membrane potential in the predepolarization and hyperpolarization-activated inward K^+ and Ca^{2+}-sensitive Cl^--currents ($I_{K,ir}$, $I_{Cl,Ca}$) regulating the spiking frequency (Grolleau and Lapied, 2000). The introduced DLC cells may have similar ionic proprieties, judging by their spike shape and frequency. Since Ca^+-channels are generally associated with synthesis and release of secretory products in the cell body, all of introduced cells are most likely neuromodulatory, too.

4.4 Neuroanatomy of descending cells in the DLC cluster

All cells have a similar projection pattern in the brain and share some morphological similarities in the suboesophageal ganglion. Some regions in the brain are innervated by all of the introduced cells. In particular, all of them provide some branching in the areas of the lateral accessory lobe and the central complex. In locust, the central complex is closely associated with the perception of the electric field vector of linearly polarized light (Heinze et al., 2009; Vitzthum et al., 2002). Furthermore it was shown that the central complex is involved in regulation of locomotion (Strauss, 2002) and spatial working memory (Neuser et al., 2008) in *Drosophila*. The region where the lateral accessory lobe (LAL), which is associated with the initiation and termination of flight in locust (Homberg, 1994), resides is a target of projections of all introduced cells. Additionally, all cells project in the peduncle of the mushroom body. Mushroombodies are generally considered as integration centre for olfactory (Kanzaki et al., 1989) and other sensory modalities, including visual (Gronenberg, 1986), acoustic (Li and Strausfeld, 1997) and

tactile (Schildberger, 1984) sensory input.

The median deutocerebrum is another area where projections of all of the introduced cells exist. Number of projecting branches and the richness of arborization in the median deutocerebrum vary between different cells. DLC Type II and V cells have only one branch with little arborization projecting into the anterior part of the deutocerebrum. However, in the DLC Type II cell lacking of finer arborization may be due to a weak staining. DLC Type III and IV cells project with several branches, reaching the tritocerebrum. Assuming that projections in the brain are mostly dendritic, some of the branches projecting in the median deutocerebrum may be already terminal outputs, because branch **I** in cells DLC Type I, III and IV splits off just after the junction from the axon descending in the nerve cord. It remains unclear what input the cells may receive in the median deutocerebrum. It could be visual because of the prominent cluster of octopaminergic cells which reside in the median deutocerebrum and are contributing to the visual dishabituation (Stern et al., 1995; Stern, 1999).

In the suboesophageal ganglion the DLC Type I-V cells share a similar neuroanatomy - their axons project either within the dorsal intermediate tract (DIT) or within the lateral dorsal tract (LDT, only DLC Type II), descending slightly in the ventral direction. Their arborizations project either in median direction, mostly in the maxillary and labial neuromeres (DLC Type I and IV), or additionally laterally, related to the position of the axon in the ganglion (DLC Type III). DLC Type II and V cells show no visible arborization pattern, probably due to a poor staining in the suboesophageal ganglion. However, their axons descends in ventral direction, too, while approaching the posterior end of the suboesophageal ganglion. It is not clear, what kind of connections to other cells DLC Type I, III and IV cells may form in the suboesophageal ganglion. The suboesophageal ganglion is considered being a higher motor centre, involved into maintenance of walking and bilateral synchronisation of motor patterns (Kien and Altman, 1984), though its exact role remains uncertain. Additionally, a number of ascending and descending DUM interneurones was identified in the suboesophageal ganglion (Bräunig and Burrows, 2004). They may represent possible projection target for DLC cells.

Only 2 cells – DLC Type I and IV were stained in the prothoracic ganglion. The structures of the DLC Type I cell are weakly stained, however, both show the similar arborization pattern with a ring-shaped arborization symmetrically on the sagittal projection. It is formed by lateral arborizations from the descending axon and one char-

acteristic branch projecting in contralateral direction, responsible for the symmetric shape of the projection.

None of the introduced cells could be stained beyond the prothoracic ganglion.

4.5 Response to stimulation

All DLC cells tested for input (DLC Type I, II, IV and V) show an increase of spike frequency after an abdominal stimulation – on both ipsi- and contralateral side, if they were stimulated separately (DLC Type I, IV, V). Tactile thoracic stimulation increased spike frequency only in the DLC Type I and V cells. Tactile stimulation of legs increased the spike frequency in the recorded in DLC Type IV cell after the stimulation of the ipsilateral hind leg and both contra- and ipsilateral middle legs and in the DLC Type V cell for all legs except the ipsilateral front leg. Tactile antennal input was inhibitory in the DLC Type II on both side of the body and in the DLC Type IV cell on the contralateral side of the body. The DLC Type V cell increased the spike frequency after both ipsi- and contralateral antennal stimulation.

Slow rhythmic pattern occurred in the DLC Type I cell. It is most likely generated in rhythm with the respiratory activity, as described by Burrows (1996). Additionally, the rhythmic activity hyperpolarized the cell by 10 mV over the recorded time span of 7 min. This leaves uncertain, whether the cell increases spiking frequency in response to some of the stimulations, since it depends on whether the stimulation was done in the hyperpolarized or depolarized part of the cycle. However, abdomen was stimulated before the onset of rhythmic activity and showed an increase of spiking frequency on both sides (fig: 3.8).

In general, a stronger input from a specific side of the body seems to exist in some of the cells: in the DLC Type IV cell for input from the ipsilateral side of the body and in the DLC Type V cell for input from the contralateral side of the body. However, such a difference is difficult to evaluate in manual stimulation, since the strength of response may depend on the applied pressure and duration of the stroke.

4.6 Function of the descending DLC I-IV cells

In locust the function of these cells is still unclear. Based on their spike properties and octopamine immunoreactivity of the DLC cluster they are most likely neuromodulatory interneurones, since their terminal projections never enter peripheral nerves in stained ganglia. Their projection sites in the brain overlap with projections of ascending suboesophageal DUM cells, especially with DUM SA 1 and 2 cells (Braunig, 1991). In *Drosphila* suboesophageal DUM cells are known to regulate aggression (Zhou et al., 2008). It was argued that they may even regulate social aggressive behaviour. Given the fact, that at least two of the introduced DLC cells should be octopaminergic, these cells may be general arousal detectors, collecting mechanosensory input from the whole body and altering the strength of response to sensory stimulation. They may represent the part of the octopaminergic system which is involved into regulation of aggression and stress response by altering the response strength to stimuli in thoracic and abdominal parts of the nerve cord. In the suboesophageal ganglion they may act as part of the feedback loop which integrates various sensory input and provides their summary as neuromodulatory output to suboesophageal and thoracic DUM cells, allowing the animal the proper behavioural and physiological response in extended stressful situations.

4.7 Conclusion

In this work, descending cells from the dorsolateral cluster in locust were characterized with respect to their anatomy and electrical properties. In four of them, evaluation of their response to sensory stimulation was performed. Since only five cells were reported to descend further than suboesophageal ganglion in the nerve cord, the five introduced cells characterize the whole known population of descending cells in the DLC.

These cells have cell bodies which are among the largest in the DLC and project within brain to the regions of central complex, lateral deutocerebrum and the peduncle of the mushroom body. Additionally, some of them project to the lateral accessory lobe and the antennal lobe. DLC Type I-III and V cells are slow-spiking cells and are, most likely, neuromodulatory interneurones.

DLC cells receive mechanosensory input. It varies between cells of different type, but all cells tested for sensory input received excitatory mechanosensory input from the abdomen. The function of these cells is still unclear, but they may function as general

arousal detectors and regulate aggression and stress response.

4.8 Future work

Future studies should investigate, which of the cells introduced in the single cell intracellular recordings are octopaminergic. A combined protocol for anti-octopamine immunocytochemistry and stainings with neurobiotin seems to be the only way to clarify this issue, since the DLC Type I-III cells share a similar morphology, size of the cell bodies and their position in the brain.

An effort should be put into staining these cells in full length. Five cells were stained and characterized, but only 4 of them descend to the 5th abdominal ganglion (and probably, further within the nerve cord). Additionally, projection pattern in the meso-, metathoracic and abdominal ganglia is of interest since it could give additional clues about their exact function.

An automated system for stimulation could provide more insight into response pattern of these cells. It could be done with air puffs, each aimed at the specified part of the body. Such an experimental setup would allow to measure the exact strength of response for each part of the body, evaluate a possible difference between strength of response on the contra- and ipsilateral sides of the body, measure a latency (assuming that air pressure and distance are kept constant) between stimulus and response in the cell and make complex test runs with experiments on habituation and dishabituation possible.

The OA3/TA cluster in *Schistocerca gregaria* appears to be not unique among other insects. Similar cluster of octopaminergic cells were found in the honeybee *Apis melifera*, cockroach *Periplaneta americana* (Kreissl et al., 1994; Sinakevitch et al., 2005), fruitfly *Drosophila melanogaster*, blow fly *Phaenicia sericata* (Sinakevitch and Strausfeld, 2006) and hawkmoth *Mandica sexta* (Dacks et al., 2005). In the honeybee, the cluster G5 has about 7 cell bodies accompanied by 6 smaller somata, all located dorsally and laterally in relation to the antennal lobe. They project to the deutocerebrum, lateral and median protocerebrum and the region of the central complex. In the brain of the cockroach, this cluster resides in a similar position, consisting of 8-10 somata of variable size. In *Manduca sexta* a small cluster of 2 cells with octopamine-immunoreactivity was found in the lateral protocerebrum (LA cells). In *Drosophila* and *Phaenicia* clusters G5a,b are

located in the ventrolateral protocerebrum and tritocerebrum and consisting of 2 and 5 cell bodies. This comparison is based on anatomy and octopamine-immunoreactivity and does not suggest similar function in different insect species, but it would be interesting to evaluate possible similarities in morphology, response to stimulation and electrical properties with intracellular recordings from single cells and stainings.

Abstract

In the dorsolateral area of the brain of the locust *Schistocerca gregaria* two descending octopaminergic cells were identified by Kononenko et al. (2009). Later studies showed, that these cells are part of a bigger cluster with five of them descend to at least, the prothoracic ganglion and four to the 4th abdominal ganglion.

In this work the dorsolateral cluster in the brain was characterized with respect to the count of cells and their size. Retrograde stainings were performed between the 5th and 4th abdominal ganglia, combined with anti-tyramine and anti-octopamine stainings to evaluate the size and number of descending and octopaminergic cells with four of them found to be descending to, at least, the 5th abdominal ganglion.

Furthermore, all five known descending cells from the dorsolateral cluster in locust were stained and characterized with respect to their anatomy and electrical properties. In four of them, initial evaluation of their response to sensory stimulation was performed. These cells have cell bodies which are among the largest in the DLC and project within brain to the regions of central complex, lateral deutocerebrum and the peduncle of the mushroom body. Additionally, some of them project to the lateral accessory lobe and the antennal lobe. Most of them are slow-spiking cells with a characteristic spike shape, being, most likely, neuromodulatory interneurons.

DLC cells receive mechanosensory input from different parts of the body. Exact pattern of mechanosensory input varies between cells of different type, but all cells tested for sensory input received excitatory mechanosensory input from the abdomen.

The function of these cells is still unclear, but they may function as general arousal detectors and regulate aggression and stress response.

Zusammenfassung

Zwei dorsolaterale oktopaminerge Zellen wurden im Gehirn von *Schistocerca gregaria* von Kononenko et al. (2009) gefunden. Spätere Untersuchungen haben gezeigt, dass sie Teil von einer größeren Gruppe von Zellen sind. Fünf von ihnen steigen ab bis, zumindest, dem prothorakalen Ganglion und vier bis zum vierten abdominalen Ganglion.

In dieser Arbeit wurde die dorsolaterale Gruppe von Zellen (DLC) im Gehirn von *Schistocerca gregaria* in Hinsicht auf die Anzahl der Zellen und ihre Größe untersucht. Retrograde Färbungen, kombiniert mit anti-Oktopamin- und anti-Tyramin-Färbungen, wurden zwischen dem vierten und dem fünften abdominalen Ganglien vorgenommen, um über die Anzahl und die Größe der absteigenden und der oktopaminergen Zellen Übersicht zu gewinnen. Es wurde festgestellt, dass 4 Zellen aus der dorsolateralen Gruppe mindestens bis zum fünften abdominalen Ganglion absteigen.

Alle fünf bekannten absteigenden Zellen in der dorsolateralen Gruppe wurden gefärbt und im Bezug auf ihre Neuroanatomie und die elektrischen Eigenschaften charakterisiert. In vier von den Zellen wurde zudem die Antwort der Zelle auf sensorische Reize untersucht. Die Zellkörper dieser Zellen gehören zu den größten unter den Zellen der dorsolateralen Gruppe. Sie haben Fortsätze im medianen Deutocerebrum, den Pilzkörpern und dem Zentralkompex des Gehirns (CC). Manche von den Zellen bilden Fortsätze in dem Antennallobus und dem LAL. Die untersuchten Zellen zeigen eine langsame Feuerrate und ihre Aktionspotentiale haben eine charakteristische Form mit einer prominenten Hyperpolarisation, was eine neuromodulatorische Wirkung vorschlägt. Sie erhalten mechanosensorischen Eingang von unterschiedlichen Körperteilen. Allerdings bekommen alle von den auf die sensorischen Eingänge untersuchten Zellen erregenden mechanosensorischen Eingang von dem Abdomen.

Die Rolle und Funktion dieser Zellen ist immer noch unklar. Es könnten absteigende neuromodulatorische Interneurone sein, die unterschiedlichen mechanosensorischen Eingang in einer Stress-relevanten Antwort bündeln.

Bibliography

Adamo, S., Linn, C., and Hoy, R. (1995).
The role of neurohormonal octopamine during 'fight or flight' behaviour in the field cricket *Gryllus bimaculatus*.
Journal of Experimental Biology, 1700:1691–1700.

Armstrong, G. A. B., Shoemaker, K. L., Money, T. G. A., and Robertson, R. M. (2006).
Octopamine mediates thermal preconditioning of the locust ventilatory central pattern generator via a cAMP/protein kinase A signaling pathway.
The Journal of Neuroscience, 26(47):12118–12126.

Bacon, J. P., Thompson, K. S., and Stern, M. (1995).
Identified octopaminergic neurons provide an arousal mechanism in the locust brain.
Journal of Neurophysiology, 74(6):2739–2743.

Bellah, K. L., Fitch, G. K., and Kammer, A. E. (1984).
A central action of octopamine on ventilation frequency in *Corydalus cornutus*.
Journal of Experimental Zoology, 231(2):289–292.

Boyan, G., Williams, L., and Herbert, Z. (2010).
Multipotent neuroblasts generate a biochemical neuroarchitecture in the central complex of the grasshopper Schistocerca gregaria.
Cell and Tissue Research, 340(1):13–28.

Boyan, G. S., Williams, J. L. D., and Ball, E. E. (1989).
The wind-sensitive cercal receptor/giant interneurone system of the locust, *Locusta migratoria*.
Journal of Comparative Physiology A, 165(4):495–510.

Braunig, P. (1991).
Suboesophageal DUM neurons innervate the principal neuropiles of the locust brain.
Philosophical Transactions of the Royal Society B: Biological Sciences, 332(1264):221–240.

Bräunig, P. and Burrows, M. (2004).
Projection patterns of posterior dorsal unpaired median neurons of the locust subesophageal ganglion.
The Journal of Comparative Neurology, 478(2):164–75.

Bräunig, P. and Eder, M. (1998).
Locust dorsal unpaired median (DUM) neurones directly innervate and modulate hindleg proprioceptors.
The Journal of Experimental Biology, 201:3333–3338.

Bräunig, P. and Pflüger, H.-J. (2001).
The unpaired median neurons of insects.
Advances in Insect Physiology, 28:185–266.

Brembs, B., Christiansen, F., Pflüger, H. J., and Duch, C. (2007).
Flight initiation and maintenance deficits in flies with genetically altered biogenic amine levels.
The Journal of Neuroscience, 27(41):11122–11131.

Broadley, K. J. (2010).
The vascular effects of trace amines and amphetamines.
Pharmacology and Therapeutics, 125(3):363–375.

Burrows, M. (1996).
The neurobiology of an insect brain.
Oxford University Press Oxford.

Christensen, T. A. and Carlson, A. D. (1982).
The neurophysiology of larval firefly luminescence: Direct activation through four bifurcating (DUM) neurons.
Journal of Comparative Physiology A, 148(4):503–514.

Cole, S. H., Carney, G. E., McClung, C. A., Willard, S. S., Taylor, B. J., and Hirsh, J. (2005).
Two functional but noncomplementing *Drosophila* tyrosine decarboxylase genes: Distinct roles for neural tyramine and octopamine in female fertility.
Journal of Biological Chemistry, 280(15):14948–14955.

Dacks, A. M., Christensen, T. a., Agricola, H.-J., Wollweber, L., and Hildebrand, J. G. (2005).

Octopamine-immunoreactive neurons in the brain and subesophageal ganglion of the hawkmoth *Manduca sexta*.
The Journal of Comparative Neurology, 488(3):255–68.

Davenport, A. P. and Evans, P. D. (2008).
Changes in haemolymph octopamine levels associated with food deprivation in the locust, *Schistocerca gregaria*.
Physiological Entomology, 3(9):269 – 274.

Donini, A. and Lange, A. B. (2004).
Evidence for a possible neurotransmitter/neuromodulator role of tyramine on the locust oviducts.
Journal of Insect Physiology, 50(4):351–61.

Downer, R. G. H., Hiripi, L., and Juhos, S. (1993).
Characterization of the tyraminergic system in the central nervous system of the locust, *Locusta migratoria migratoides*.
Neurochemical Research, 18(12):1245–1248.

Duch, C. and Pflüger, H. J. (1999).
DUM neurons in locust flight: A model system for amine-mediated peripheral adjustments to the requirements of a central motor program.
Journal of Comparative Physiology A, 184(5):489–499.

Erspamer, V. (1948).
Active substances in the posterior salivary glands of octopoda. I. Enteraminelike substance.
Acta Pharmacologica et Toxicologica, (Henze 1913):213–223.

Esparmer, V. and Boretti, G. (1951).
Identification and characterization, by paper chromatography, of enteramine, octopamine, tyramine, histamine and allied substances in extracts of posterior salivary glands of octopoda and in other tissue extracts of vertebrates and invertebrates.
Archives Internationales de Pharmacodynamie et de Therapie, 88(3):296–332.

Evans, P. D. and O'Shea, M. (1977).
An octopaminergic neurone modulates neuromuscular transmission in the locust.
Nature, 270(5634):257–259.

Evans, P. D. and Siegler, M. V. (1982).
Octopamine mediated relaxation of maintained and catch tension in locust skeletal muscle.
The Journal of Physiology, 324(1):93–112.

Farooqui, T. (2012).
Review of octopamine in insect nervous systems.
Open Access Insect Physiology, pages 1–17.

Goodman, C. S., Pearson, K. G., and Spitzer, N. C. (1980).
Electrical excitability: a spectrum of properties in the progeny of a single embryonic neuroblast.
Proceedings of the National Academy of Sciences, 77(3):1676–80.

Grolleau, F. and Lapied, B. (2000).
Dorsal unpaired median neurones in the insect central nervous system: towards a better understanding of the ionic mechanisms underlying spontaneous electrical activity.
Journal of Experimental Biology, 203(11):1633–48.

Gronenberg, W. (1986).
Physiological and anatomical properties of optical input-fibres to the mushroom body in the bee brain.
Journal of Insect Physiology, 32(8):695–704.

Gruntenko, N., Chentsova, N. A., Bogomolova, E. V., Karpova, E. K., Glazko, G. V., Faddeeva, N. V., Monastirioti, M., and Rauschenbach, I. Y. (2004).
The effect of mutations altering biogenic amine metabolism in *Drosophila* on viability and the response to environmental stresses.
Archives of Insect Biochemistry and Physiology, 55(2):55–67.

Hammer, M. (1993).
An identified neuron mediates the unconditioned stimulus in associative olfactory learning in honeybees.
Nature, 366(6450):59–63.

Hardie, S. L., Zhang, J. X., and Hirsh, J. (2007).
Trace amines differentially regulate adult locomotor activity, cocaine sensitivity, and female fertility in *Drosophila melanogaster*.

Developmental Neurobiology, 67(10):1396–1405.

Heinze, S., Gotthardt, S., and Homberg, U. (2009).
Transformation of polarized light information in the central complex of the locust.
The Journal of Neuroscience, 29(38):11783–93.

Hirashima, A. and Eto, M. (1993).
Effect of stress on levels of octopamine, dopamine and serotonin in the American cockroach (*Periplaneta americana L.*).
Comparative Biochemistry and Physiology C, 105(2):279–284.

Homberg, U. (1994).
Flight-correlated activity changes in neurons of the lateral accessory lobes in the brain of the locust *Schistocerca gregaria*.
Journal of Comparative Physiology A, 175(5):597–610.

Homberg, U., Hofer, S., Pfeiffer, K., and Gebhardt, S. (2003).
Organization and neural connections of the anterior optic tubercle in the brain of the locust, *Schistocerca gregaria*.
The Journal of Comparative Neurology, 462(4):415–430.

Hustert, R. (1978).
Segmental and interganglionic projections from primary fibres of insect mechanoreceptors.
Cell and Tissue Research, 194:337–351.

Jia, X. X. and Siegler, M. V. S. (2002).
Midline lineages in grasshopper produce neuronal siblings with asymmetric expression of Engrailed.
Development, 129(22):5181–93.

John W. Eaton David Bateman, S. H. and Wehbring, R. (2014).
GNU Octave version 3.8.1 manual: a high-level interactive language for numerical computations.
CreateSpace Independent Publishing Platform.

Kanzaki, R., Arbas, E. A., Strausfeld, N. J., and Hildebrand, J. G. (1989).
Physiology and morphology of projection neurons in the antennal lobe of the male moth *Manduca sexta*.
Journal of Comparative Physiology A, 165(4):427–453.

Kien, J. and Altman, J. S. (1984).
Descending interneurones from the brain and suboesophageal ganglia and their role in the control of locust behaviour.
Journal of Insect Physiology, 30(1):59–72.

Kita, H. and Armstrong, W. (1991).
A biotin-containing compound N-(2-aminoethyl)biotinamide for intracellular labeling and neuronal tracing studies: comparison with biocytin.
Journal of Neuroscience Methods, 37(2):141–50.

Konings, P. N. M., Vullings, H. G. B., Geffard, M., Buijs, R. M., Diederen, J. H. B., and Jansen, W. F. (1988).
Immunocytochemical demonstration of octopamine-immunoreactive cells in the nervous system of *Locusta migratoria* and *Schistocerca gregaria*.
Cell and Tissue Research, 251(2):371–379.

Kononenko, N. L., Wolfenberg, H., and Pflüger, H.-J. (2009).
Tyramine as an independent transmitter and a precursor of octopamine in the locust central nervous system: an immunocytochemical study.
The Journal of Comparative Neurology, 512(4):433–52.

Kreissl, S., Eichmüller, S., Bicker, G., Rapus, J., and Eckert, M. (1994).
Octopamine-like immunoreactivity in the brain and subesophageal ganglion of the honeybee.
The Journal of Comparative Neurology, 348(4):583–95.

Kutsukake, M., Komatsu, A., Yamamoto, D., and Ishiwa-Chigusa, S. (2000).
A tyramine receptor gene mutation causes a defective olfactory behavior in *Drosophila melanogaster*.
Gene, 245(1):31–42.

Lewin, A. H. (2008).
Receptors of mammalian trace amines.
Drug Addiction: From Basic Research to Therapy, 8(1):327–339.

Li, Y. and Strausfeld, N. J. (1997).
Morphology and sensory modality of mushroom body extrinsic neurons in the brain of the cockroach, *Periplaneta americana*.
The Journal of Comparative Neurology, 387(4):631–650.

Matsushita, T., Kuwasawa, K., Uchimura, K., Ai, H., and Kurokawa, M. (2002).
Biogenic amines evoke heartbeat reversal in larvae of the sweet potato hornworm, *Agrius convolvuli*.
Comparative Biochemistry and Physiology A, 133(3):625–636.

Mentel, T., Duch, C., Stypa, H., Wegener, G., Müller, U., and Pflüger, H.-J. (2003).
Central modulatory neurons control fuel selection in flight muscle of migratory locust.
The Journal of Neuroscience, 23(4):1109–1113.

Monastirioti, M. (2003).
Distinct octopamine cell population residing in the CNS abdominal ganglion controls ovulation in *Drosophila melanogaster*.
Developmental Biology, 264(1):38–49.

Monastirioti, M., Linn, C. E., and White, K. (1996).
Characterization of *Drosophila* tyramine beta-hydroxylase gene and isolation of mutant flies lacking octopamine.
The Journal of Neuroscience, 16(12):3900–11.

Nagaya, Y. (2002).
A trace amine, tyramine, functions as a neuromodulator in *Drosophila melanogaster*.
Neuroscience Letters, 329(3):324–328.

Neuser, K., Triphan, T., Mronz, M., Poeck, B., and Strauss, R. (2008).
Analysis of a spatial orientation memory in *Drosophila*.
Nature, 453(7199):1244–1247.

Orchard, I. (1982).
Octopamine in insects: neurotransmitter, neurohormone, and neuromodulator.
Canadian Journal of Zoology, 60(4):659–669.

Orchard, I., Carlisle, J. A., Loughton, B. G., Gole, J. W., and Downer, R. G. (1982).
In vitro studies on the effects of octopamine on locust fat body.
General and Comparative Endocrinology, 48(1):7–13.

Orchard, I. and Lange, A. B. (1984).
Cyclic AMP in locust fat body: Correlation with octopamine and adipokinetic hormones during flight.
Journal of Insect Physiology, 30(12):901–904.

Orchard, I. and Lange, A. B. (1985).
Evidence for octopaminergic modulation of an insect visceral muscle.
Journal of Neurobiology, 16(3):171–181.

Orchard, I., Ramirez, J.-M. M., and Lange, A. B. (1993).
A multifunctional role for octopamine in locust flight.
Annual Review of Entomology, 38(1):227–249.

Pflüger, H. J. and Stevenson, P. A. (2005).
Evolutionary aspects of octopaminergic systems with emphasis on arthropods.
Arthropod Structure and Development, 34(3):379–396.

Platt, N. and Reynolds, S. E. (1986).
The pharmacology of the heart of a caterpillar, the tobacco hornworm, *Manduca sexta*.
Journal of Insect Physiology, 32(3):221–230.

Plotnikova, S. I. (1969).
Effector neurons with several axons in the ventral nerve cord of the asian grasshopper *Locusta migratoria*.
Journal of Evolutionary Biochemistry and Physiology, 5:276–277.

Pouzat, C. and Chaffiol, A. (2009).
Automatic spike train analysis and report generation. An implementation with R, R2HTML and STAR.
Journal of Neuroscience Methods, 181(1):119–44.

R Core Team (2016).
R: A Language and Environment for Statistical Computing.
R Foundation for Statistical Computing, Vienna, Austria.

Ramirez, J.-M. and Orchard, I. (1990).
Octopaminergic modulation of the forewing stretch receptor in the locust *Locusta migratoria*.
Journal of Experimental Biology, 149:255–279.

Schildberger, K. (1984).
Multimodal interneurons in the cricket brain: properties of identified extrinsic mushroom body cells.
Journal of Comparative Physiology A, 154(1):71–79.

Schindelin, J., Arganda-Carreras, I., Frise, E., Kaynig, V., Longair, M., Pietzsch, T., Preibisch, S., Rueden, C., Saalfeld, S., Schmid, B., Tinevez, J.-Y., White, D. J., Hartenstein, V., Eliceiri, K., Tomancak, P., and Cardona, A. (2012).
Fiji: an open-source platform for biological-image analysis.
Nature Methods, 9(7):676–682.

Schwaerzel, M., Monastirioti, M., Scholz, H., Friggi-Grelin, F., Birman, S., and Heisenberg, M. (2003).
Dopamine and octopamine differentiate between aversive and appetitive olfactory memories in *Drosophila*.
The Journal of Neuroscience, 23(33):10495–10502.

Sinakevitch, I., Niwa, M., and Strausfeld, N. J. (2005).
Octopamine-like immunoreactivity in the honey bee and cockroach: Comparable organization in the brain and subesophageal ganglion.
The Journal of Comparative Neurology, 488(3):233–254.

Sinakevitch, I. and Strausfeld, N. J. (2006).
Comparison of octopamine-like immunoreactivity in the brains of the fruit fly and blow fly.
The Journal of Comparative Neurology, 494(3):460–475.

Stern, M. (1999).
Octopamine in the locust brain: cellular distribution and functional significance in an arousal mechanism.
Microscopy Research and Technique, 45(3):135–41.

Stern, M., Thompson, K. S. J., Zhou, P., Watson, D. G., Midgley, J. M., Gewecke, M., and Bacon, J. P. (1995).
Octopaminergic neurons in the locust brain: morphological, biochemical and electrophysiological characterisation of potential modulators of the visual system.
Journal of Comparative Physiology A, 177(5):611–625.

Stevenson, P. A. (1999).
Colocalisation of taurine- with transmitter-immunoreactivities in the nervous system of the migratory locust.
The Journal of Comparative Neurology, 404(1):86–96.

Stevenson, P. A. (2005).

Octopamine and experience-dependent modulation of aggression in crickets.
The Journal of Neuroscience, 25(6):1431–1441.

Stevenson, P. A., Pflüger, H. J., Eckert, M., and Rapus, J. (1992).
Octopamine immunoreactive cell populations in the locust thoracic-abdominal nervous system.
The Journal of Comparative Neurology, 315(4):382–97.

Stevenson, P. A., Pflüger, H. J., Eckert, M., and Rapus, J. (1994).
Octopamine-like immunoreactive neurones in locust genital abdominal ganglia.
Cell and Tissue Research, 275(2):299–308.

Strauss, R. (2002).
The central complex and the genetic dissection of locomotor behaviour.
Current Opinion in Neurobiology, 12(6):633–638.

Taghert, P. H. and Goodman, C. S. (1984).
Cell determination and differentiation of identified serotonin-immunoreactive neurons in the grasshopper embryo.
The Journal of Neuroscience, 4(4):989–1000.

Thompson, K. J. and Siegler, M. V. (1993).
Development of segment specificity in identified lineages of the grasshopper CNS.
The Journal of Neuroscience, 13(8):3309–18.

Tyrer, N. M. and Gregory, G. E. (1982).
A guide to the neuroanatomy of locust suboesophageal and thoracic ganglia.
Philosophical Transactions of the Royal Society B, 297(1085):91–123.

Van der Horst, D. J., Van Marrewijk, W. J. A., and Diederen, J. H. B. (2001).
Adipokinetic hormones of insect: Release, signal transduction, and responses.
International Review of Cytology, 211:179–240.

Van Marrewijk, W., Van den Broek, A., and Beenakkers, A. (1980).
Regulation of glycogenolysis in the locust fat body during flight.
Insect Biochemistry, 10(6):675–679.

Vitzthum, H., Muller, M., and Homberg, U. (2002).
Neurons of the central complex of the locust *Schistocerca gregaria* are sensitive to polarized light.

The Journal of Neuroscience, 22(3):1114–1125.

Vladimirov, V., Thiselton, D. L., Kuo, P.-H., McClay, J., Fanous, A., Wormley, B., Vittum, J., Ribble, R., Moher, B., van den Oord, E., O'Neill, F. A., Walsh, D., Kendler, K. S., and Riley, B. P. (2007).
A region of 35 kb containing the trace amine associate receptor 6 (TAAR6) gene is associated with schizophrenia in the Irish study of high-density schizophrenia families.
Molecular Psychiatry, 12(9):842–853.

Zhou, C., Rao, Y., and Rao, Y. (2008).
A subset of octopaminergic neurons are important for *Drosophila* aggression.
Nature Neuroscience, 11(9):1059–67.